Mon. Not. R. Astron. Soc. **000**, 000–000 (0000) Printed 21 April 2014 (MN LATEX style file v2.2)

The catalogues and mid-infrared environment of Interstellar OH Masers

Haihua Qiao[1,2,3,4⋆], Juan Li[1,4], Zhiqiang Shen[1,3,4], Xi Chen[1,3,4], Xingwu Zheng[5,6]
[1] *Shanghai Astronomical Observatory, Chinese Academy of Sciences, 80 Nandan Road, Shanghai, China, 200030*
[2] *University of Chinese Academy of Sciences, 19A Yuquanlu, Beijing, China, 100049*
[3] *Key Laboratory for Research in Galaxies and Cosmology, Shanghai Astronomical Observatory, Chinese Academy of Sciences, 80 Nandan Road, Shanghai, China, 20030*
[4] *Key Laboratory of Radio Astronomy, Chinese Academy of Science, 80 Nandan Road, Shanghai, China, 200030*
[5] *School of Astronomy & Space Science, Nanjing University, 22 Hankou RD, Jiangsu Province, China, 210093*
[6] *Key Laboratory of Modern Astronomy and Astrophysics (Nanjing University), Ministry of Education, Jiangsu Province, China, 210093*

arXiv:1404.4677v1 [astro-ph.GA] 18 Apr 2014

21 April 2014

ABSTRACT

Data for a number of OH maser lines have been collected from surveys. The positions are compared to recent mid-infrared (MIR) surveys such as *Spitzer*-GLIMPSE and *WISE*, restricting the comparison to point sources. The colors and intensities of the IR sources are compared. There are many 18 cm OH masers, but far fewer in lines arising from higher energy levels. We also make a comparison with the 5 cm Class II methanol masers. We have divided the results into 3 subsamples: those associated with OH masers only, those associated with OH masers and Class II methanol masers, and those only associated with Class II methanol masers. There are no obvious differences in the color-color or color-magnitude results for the GLIMPSE point sources. However, according to the results from the *WISE* 22 μm survey, the sources associated with OH masers are brighter than those associated with methanol masers. We interpret the presence of OH and methanol masers mark the locations of regions where stars are forming. The OH masers are located on the borders of sharp features found in the IR. These are referred to as bubbles. If the OH masers mark the positions of protostars, the result provides indirect evidence for triggered star formation caused by the expansion of the bubbles.

Key words: methods: statistical - masers - stars: formation - ISM: bubbles.

1 INTRODUCTION

Interstellar Hydroxyl (OH) masers are an important tool for probing the environment of massive star-forming regions (SFRs). The maser phase is contemporaneous with the evolution of an ultra-compact (UC) HII region around the star (Reid 2002), but dies out rapidly when the HII region has enlarged to a size greater than 30 milliparsec (mpc) (Caswell 2001). Thus the masers offer a means to discover the star at its early stage when it is hidden from the dust in the surrounding molecular clouds. Some recent interferometric observations, e.g. Migenes et al. (2005), Fish & Sjouwerman (2007), Harvey-Smith & Cohen (2007), Bains et al. (2008), and Slysh et al. (2010), provide high spectral resolutions and high positional accuracies, which are used to study the origins of the maser flares, maser velocity structures, and measure the magnetic strength in the SFRs. These studies shed new light on small-scale maser process and help us to understand the physical environment of the SFRs.

OH maser emission from the ground-state transitions ($^2\Pi_{3/2}$, $J = 3/2$ state) was firstly found toward several galactic HII regions (e.g. W3(OH)) by Weaver et al. (1965) and Gundermann (1965). The 1665/1667 MHz ground-state transitions in SFRs are usually the strongest OH masers. They are generally accompanied by the weaker OH masers of other transitions, e.g. at excited transitions of $^2\Pi_{1/2}$, $J = 1/2$ and $^2\Pi_{3/2}$, $J = 5/2$. The excited state of OH ($^2\Pi_{1/2}$, $J = 1/2$ state) at 4765 MHz was firstly detected in the source W3(OH) and W49N (Zuckerman et al. 1968). The first detection of the excited state of OH ($^2\Pi_{3/2}$, $J = 5/2$ state) at 5 cm wavelength (6035 MHz) was made by Yen et al. (1969) toward W3. The highly excited state of OH ($^2\Pi_{3/2}$, $J = 7/2$ state) at 13441.417 MHz ($F = 4 - 4$)

⋆ E-mail:qiaohh@shao.ac.cn

© 0000 RAS

was discovered by Turner et al. (1970) in the W3(OH). The line radiation of excited OH (e.g. $^2\Pi_{1/2}$, $J = 1/2$ state; $^2\Pi_{3/2}$, $J = 5/2$ state; $^2\Pi_{3/2}$, $J = 7/2$ state) is particularly helpful in complementing the ground-state observations to understand the maser pumping process and interpret the physical conditions that are implied by the presence of the masers (Caswell 2001). Extensive OH maser searches have been carried out toward color-selected infrared (IR) sources, or known SFRs associated with CH_3OH masers (e.g. Cohen et al. 1991; Cohen et al. 1995; Edris et al. 2007). These observations resulted in detections of hundreds of interstellar OH masers and supply an important tool for studies of maser pumping and physical conditions of their host SFRs (e.g. Szymczak et al. 2000; Szymczak & Gérard 2004). However, until now there are no complete catalogues of all detected interstellar OH masers at each of the detected transitions. Mu et al. (2010) collected 3249 OH maser sources at 18 cm wavelength from the literature published up to April 2007, but the majority of the sources are stellar OH masers. Therefore, we performed an extensive literature search and compiled a complete catalogue of the detected interstellar OH masers so far.

The evolutionary phase that the interstellar OH masers trace the evolutionary sequence for different species of masers is still unclear now. Ellingsen (2006) examined the mid-infrared (MIR) properties of methanol masers with or without associated OH masers using the *Spitzer* Galactic Legacy Infrared Mid-Plane Survey Extraordinaire (GLIMPSE) point source data. He proposed that OH masers may be generally associated with a later evolutionary phase or the stellar mass range associated with OH masers extends to higher masses than for methanol masers. However, because of the small numbers in each sample in Ellingsen (2006), more data and investigations are needed to give firm conclusions. From this consideration, we make use of the GLIMPSE point source data to extensively study the MIR environment of the interstellar OH masers from larger size samples of OH and methanol masers. GLIMPSE is a legacy science program of the *Spitzer* Space Telescope which covered the inner Galactic plane ($|l| \leqslant 65^\circ$) at 3.6, 4.5, 5.8, 8.0 μm MIR wavelength bands with 1.4″-1.9″ resolutions, with the Infrared Array Camera (IRAC; Benjamin et al. 2003). As such, it offers us the best opportunity to study the MIR environment of interstellar OH masers and compare them with other sources. In addition, we also investigate the MIR environment of interstellar OH masers with the data from Wide-field Infrared Survey Explorer (*WISE*) survey which mapped the full sky at 3.4, 4.6, 12 and 22 μm with an angular resolution of 6.1″, 6.4″, 6.5″, 12″ in the four bands, respectively (Wright et al. 2010). *WISE* can provide more information about the MIR environment of interstellar OH masers at longer MIR wavelengths which are complementary and important for our study. The *Spitzer*-GLIMPSE images at 8.0 μm revealed "a bubbling Galactic disk" (Churchwell et al. 2006; Churchwell et al. 2007). MIR bubbles are important and widespread morphological features in the interstellar medium (ISM). Bubbles could trigger the massive-star formation. During the expansion of the bubbles, neutral material accumulates on the border of bubbles, and becomes very massive with time. A new generation of stars may form in the collected layer (Deharveng et al. 2010). In this case, OH masers are possibly associated with bubbles and might be found on the boarders of bubbles. Therefore, we investigate the relationship between OH masers and bubbles.

This paper is organised as follows. In Section 2, we introduce the data description. In Section 3, we describe the catalogues and present the relationship of flux densities between 18 cm OH masers and 5 cm OH masers. In Section 4, we discuss the IR environment of the interstellar OH masers, followed by a summary in Section 5.

2 DATA DESCRIPTION

2.1 Ground-state OH maser surveys

Before the 1990's, ground-state OH maser surveys were mostly made with single-dish antennae, having rms position uncertainties greater than 10″ (e.g. Caswell et al. 1980; Caswell & Haynes 1983; Caswell & Haynes 1987). In the 1990's, interferometric OH maser surveys were carried out to obtain subarcsecond position accuracy. These observations include Caswell (1998) (hereafter C98), Forster & Caswell (1999) (hereafter FC99), and Caswell (1999) (hereafter C99). Caswell (1998, 1999) used the Australia Telescope Compact Array (ATCA) to measure the positions for all the detected 18 cm OH masers before those two observaitons. With the Very Large Array (VLA), Forster & Caswell (1999) presented the positions and spectra of 1665 MHz OH masers in 74 SFRs which were known to contain OH masers.

In the 2000's, some targeted surveys were made by Argon et al. (2000) (hereafter A2000), Szymczak & Gérard (2004) (hereafter SG2004) and Edris et al. (2007) (hereafter EF2007) with single-dish or interferometric instruments. Argon et al. (2000) observed 396 sources which have maser emission in OH and/or H_2O with NRAO 43 m telescope in Green Bank, obtained 91 interstellar OH masers with peak flux densities stronger than 1 Jy in both circular polarizations and finally mapped them with VLA. Szymczak & Gérard (2004) made the observations of OH ground-state transitions in 100 methanol maser sources with the Nançay radio telescope, resulting in 55 OH maser detections. The detection rate of 55% is the highest one in all targeted surveys for ground-state OH masers. Edris et al. (2007) observed 217 IRAS point sources exhibiting IR colors of high mass protostellar objects with the Nançay telescope and Green Bank Telescope (GBT), and detected 63 OH masers, 36 of which are new detections. Table 1 presents the detection rate, 1 - σ sensitivity of the observations (when reported in the associated publication), the significant decimal numbers in RA (s) and DEC (″), and the target types for all ground-state and excited-state OH maser surveys.

2.2 Excited-state OH maser surveys

2.2.1 6 cm OH maser surveys

The targets for 6 cm OH maser surveys were generally selected from the known presence of 5/6/18 cm OH masers, H_2O masers, or methanol masers. Szymczak et al. (2000) (hereafter SK2000) carried out a survey towards 57 SFRs with 6/18 cm OH masers or methanol masers, and detected

Table 1. Summary of the interstellar OH maser surveys.

Code	Telescope	Reference	#det./#obs.	1σ[Jy]	SN-RA(s)[a]	SN-DEC($''$)[b]	Selection
18 cm							
C98	ATCA	Caswell (1998)	–	0.04	2	1	18cm OH
FC99	VLA	Forster et al. (1999)	–	0.1	2	1	SFRs
C99	ATCA	Caswell (1999)	–	0.03	2	1	18cm OH
A2000	VLA	Argon et al. (2000)	91/396	0.3	2	1	18cm OH,H_2O
SG2004	Nançay	Szymczak et al. (2004)	55/100	0.04	1	0	Methanol
EF2007	Nançay,GBT,100m	Edris et al. (2007)	63/217	0.05–0.1	1	0	IRAS(MYOs)
6 cm							
CM91	Lovell,76m	Gohen et al. (1991)	9/44	0.05–0.3	1	0	IRAS(18cm OH)
CM95	Parkes,64m	Cohen et al. (1995)	5/85	0.1	2	1	IRAS,(U HII)
S97	HartRAO,26m	Smits (1997)	6/29	0.3–0.5	–	–	6/18cm OH,Methanol
SK2000	Torun,32m	Szymczak et al. (2000)	9/57	0.7	2	1	18cm OH,H_2O
DE2002	ATCA	Dodson et al. (2002)	14/55	0.02	2	1	SFRs
S2003	HartRAO,26m	Smits (2003)	3/69	0.2–0.4	1	0	18cm OH,Methanol
PG2004	VLA	Palmer et al. (2004)	–	∼0.013	2	1	6cm OH
SC2005	MERLIN	Harvey-Smith et al. (2005)	–	0.004–0.255	4	3	SFRs
5 cm							
S94	HartRAO,26m	Smits (1994)	10/257	∼0.9	–	–	OH,Methanol,H_2O
CV95	Parkes,64m	Caswell et al. (1995)	52/208	∼0.1	1	0	18 OH
BD97	Effelsberg,100m	Baudry et al. (1997)	27/165	–	2	1	18cm OH,H_2O ,IRAS
C2001	ATCA	Caswell (2001)	–	0.04	2	1	5cm OH
C2003	Parkes,64m	Caswell (2003)	–	0.03–0.05	2	1	5cm OH
2.3 cm							
BD2002	Effelsberg,100m	Baudry et al. (2002)	4/27	∼0.05	2	2	5cm OH
C2004	Parkes,64m	Caswell (2004)	8/56	∼0.022	2	1	5cm OH

[a] The significant decimal numbers for RA (s).
[b] The significant decimal numbers for DEC ($''$).

nine OH maser sources at 6 cm wavelength. Smits (2003) (hereafter S2003) detected three OH masers at 6 cm wavelength from 69 SFRs with 18 cm OH masers or methanol masers. Dodson & Ellingsen (2002) (hereafter DE2002) carried out sensitive observations of OH maser emission at 6 cm wavelength towards 55 SFRs, and discovered fourteen sources.

Far-infrared flux has also been used to compile the survey samples. Cohen et al. (1991) (hereafter CM91) chose 18 cm OH masers with strong IRAS 60 μm flux density, together with eight known 6 cm OH masers as the survey sample, and detected nine OH masers at 6 cm wavelength. Subsequent work by Cohen et al. (1995) (hereafter CM95) discovered five new OH masers at 6 cm wavelength from IRAS sources with FIR colors of UC HII regions and embedded OB stars.

Some papers about monitoring the flux density, position measurements or phase-referenced observations for 6 cm OH masers were constructed. Smits (1997) (hereafter S97) detected six OH masers at 6 cm wavelength from 29 SFRs with 6/18 cm OH masers or methanol masers, and monitored them for a period of more than a year. Palmer et al. (2004) (hereafter PG2004) used VLA to determine the precise positions for 4765 MHz OH masers and the observations were successful for four OH masers. Recently, Harvey-Smith & Cohen (2005) (hereafter SC2005) made phase-referenced observations of thirteen SFRs at 4765 MHz with the Multi-Element Radio Linked Interferometer Network (MERLIN), and had ten detections at 4765 MHz, two detections at 4750 MHz, and one detection at 4660 MHz.

2.2.2 5 cm OH maser surveys

The targets for the 5 cm OH maser surveys were selected either by the presence of maser species (18 cm OH, H_2O, methanol masers) or by IRAS point sources exhibiting colors of UC HII regions. Smits (1994) (hereafter S94) searched for 6035 MHz OH masers towards 257 SFRs with 18 cm OH, H_2O, or methanol masers, and discovered ten new maser sources. Caswell & Vaile (1995) (hereafter CV95) detected 72 masers at the 6035 MHz transition towards 208 ground-state OH masers with 1665 MHz flux density greater than 0.8 Jy, and among them, 52 OH masers were firstly detected. Baudry et al. (1997) (hereafter BD97) undertook a comprehensive search for 5 cm OH masers towards 165 sources, and detected 16 new OH masers.

Caswell (2001, 2003) (hereafter C2001, C2003) measured the positions of 5 cm OH masers with high accuracy and studied their polarization properties. He used ATCA to

measure positions for more than 50 OH masers at the 6035 MHz transition with subarcsecond accuracy and discovered eleven new masers. He also studied the circular polarization properties in the spectra of 91 previously catalogued OH masers at the 6035 and 6030 MHz transitions with the Parkes radio telescope and provided more recent information for them.

2.2.3 2.3 cm OH maser surveys

The 2.3 cm OH masers are usually searched towards 5 cm OH masers. Baudry & Desmurs (2002) (hereafter BD2002) used the Effelsberg telescope to carry out sensitive observations towards 27 compact or ultra-compact HII regions with 6035 MHz OH masers brighter than 0.5 Jy, and discovered three new masers at 13441 MHz in addition to W3(OH). Caswell (2004) (hereafter C2004) detected seven new masers at 13441 MHz from the sites of 56 catalogued 6035 MHz OH masers.

3 RESULTS

3.1 Catalogue description

The detected interstellar OH masers and their basic information are listed in Tables 2, 3, 4, 5 (The full tables containing all sources are available electronically) for 18 cm, 6 cm, 5 cm, 2.3 cm OH masers, respectively. The catalogue entries are in order of the ascending right ascension (RA). The columns in Tables 2, 3, 4, 5 are as follows (the template is shown in Table 2): (1) the catalogue number; (2) the source name (collected from the literature); (3) and (4) the OH maser position in RA and declination (DEC) (J2000), respectively; (5) the observing frequency and its polarization information (some observations only have the single-polarization information); (6) the peak velocity of OH masers (km s^{-1}); (7) the velocity range of OH masers (km s^{-1}); (8) the flux density of OH masers (Jy; for the interferometer observations, the lower limit of the flux density is given); (9) the references; (10) the alias of OH masers.

The position accuracy may be inferred from the positions presented in the catalogues. The significant decimal numbers for RA (s) and DEC ($''$) are listed in Table 1. The ATCA, VLA and some single-dish observations (C98, FC99, C99, A2000, CM95, SK2000, DE2002, PG2004, BD97, C2001, C2003, C2004) have two significant decimal numbers in RA and one in DEC. Positions from some single-dish measurements (SG2004, EF2007, CM91, S2003, CV95) have one significant decimal number in RA and none in DEC. Baudry & Desmurs (2002) (BD2002) has two significant decimal numbers in both RA and DEC. The MERLIN observations (SC2005) have four and three significant decimal numbers in RA and DEC, respectively. Not all source positions have been determined with high accuracy, and this produces some difficulties when trying to draw firm conclusions about the associations.

The determination of the flux densities and velocities is described as follows. If the OH masers are observed with interferometers, such as A2000 and FC99 data, we choose the maximum flux density as the flux density of the source (the lower limit, marked with ">") and its V_{lsr} as the peak velocity. Then we determine the velocity range based on the maximum and minimum velocities of the source. If the source has both single-polarization observation and total flux density observation, the total flux density observation is selected. If the source has been observed for many times, the observation which has higher RA and DEC accuracy or gives the accurate flux density will be adopted. Sometimes, the source has several flux densities because of variability.

3.2 The relationship between 1665 MHz flux density and 6035 MHz flux density

We use the 1665 MHz and 6035 MHz OH maser catalogues to investigate the relationship between the flux density of these two transitions. We select the OH masers, which have total flux densities (not the lower limit). In total, we have 249 sources at the 1665 MHz transition and 118 sources at the 6035 MHz transition. From Forster & Caswell (1989), Caswell (1997) and Caswell et al. (2010), if a separation between masers (assuming that they have the same distance) is greater than $6''$, these masers are not closely associated (but probably in the same stellar cluster if their velocity ranges are similar). So we take $6''$ as the separation criterion to investigate the association between these two samples, resulting in 47 sources which possess both transitions. Fig. 1 shows that there is a weak correlation between the flux density of the 1665 MHz transition and the 6035 MHz transition, which was expected by Guilloteau (1982). The range of the flux density ratio $R = S(6035)/S(1665)$ is from 6 to $\frac{1}{400}$, and the majority of sources have the R between 3 and $\frac{1}{6}$. Caswell & Vaile (1995) found that the greater the peak of 1665 MHz maser intensity is, the greater the detection rate of 6035 MHz masers is. Pavlakis & Kylafis (1996) presented a detailed pumping scheme which accounts well for the ground-state OH masers (at 18 cm transition) in SFRs and can apparently also account quite well for the 5 cm transition under similar conditions (Pavlakis & Kylafis 2000). According to their model, the 6035 MHz line is weaker than the 1665 MHz line and is pumped towards higher gas densities compared to that for the 1665 MHz line. The flux density ratio of 1665 MHz line and 6035 MHz line could be used to restrict the physical parameters of maser regions. For a line of frequency ν emitting from a source of area Ω, the flux density S is proportional to $T_b\nu^2\Omega$. In order to compare the observed flux density ratio $R = S(6035)/S(1665)$ with the model brightness temperature ratio ($T_b(6035)/T_b(1665)$), an assumption about the relative size of the maser sources are required. If the 1665 MHz maser spots and 6035 MHz maser spots are comparable in size, the flux density ratios of $R = 13$ and $R = 1$ correspond to the brightness temperature ratio of unity and $\frac{1}{13}$. Based on Cragg et al. (2002) model, we can roughly estimate the physical conditions of the maser region. For the gas kinetic temperature $T_k = 30K$, the dust temperature $T_d = 175K$, the flux density ratio $R = 13$, the hydrogen density n_H is $\sim 10^{7.8} cm^{-3}$ and the specific column density $N_{OH}/\triangle V$ (N_{OH} is the column density of OH; $\triangle V$ is the linewidth) is $\sim 10^{11.85} cm^{-3} s$; For the same conditions of gas kinetic temperature and dust temperature, but with the flux density ratio $R = 1$, the hydrogen density n_H is $\sim 10^{6.9} cm^{-3}$ and the specific column density $N_{OH}/\triangle V$ is $\sim 10^{11.00} cm^{-3} s$.

Table 2. Catalogue of 18 cm interstellar OH masers. (This table (and Table 3, Table 4, Table 5) is available in its entirety in a machine-readable form in the online journal. A portion is shown here for guidance regarding its form and content.)

No.	Source name	RA(J2000) (h m s)	DEC(J2000) (^{o} ' ")	Freq. (MHz)	Vpeak (km s^{-1})	Vrange (km s^{-1})	Flux density (Jy)	Ref.	Other name
1	G126.715-0.822	01 23 33.17	+61 48 49.2	1665L	-12.06	-12.06,-8.64	>1.50	A2000	
1	G126.715-0.822	01 23 33.17	+61 48 49.2	1665R	-5.74		>0.50	A2000	
2	G133.715+1.215	02 25 40.59	+62 05 50.5	1665L	-39.29	-43.96,-37.59	>4.31	A2000	W3
2	G133.715+1.215	02 25 40.59	+62 05 50.5	1665R	-39.2		>0.75	A2000	W3
3	G133.946+1.064	02 27 03.70	+61 52 25.4	1612L	-43.15	-47.51,-42.3	>1.68	A2000	W3 OH
3	G133.946+1.064	02 27 03.70	+61 52 25.4	1612R	-42.17	-42.92,-41.48	>6.21	A2000	W3 OH
3	G133.946+1.064	02 27 03.70	+61 52 25.4	1665L	-46.29	-48.94,-41.93	>132.32	A2000	W3 OH
3	G133.946+1.064	02 27 03.70	+61 52 25.4	1665R	-45.02	-48.9,-40.02	>200.54	A2000	W3 OH
3	G133.946+1.064	02 27 03.70	+61 52 25.4	1667L	-44.43	-47.77,-43.31	>26.87	A2000	W3 OH

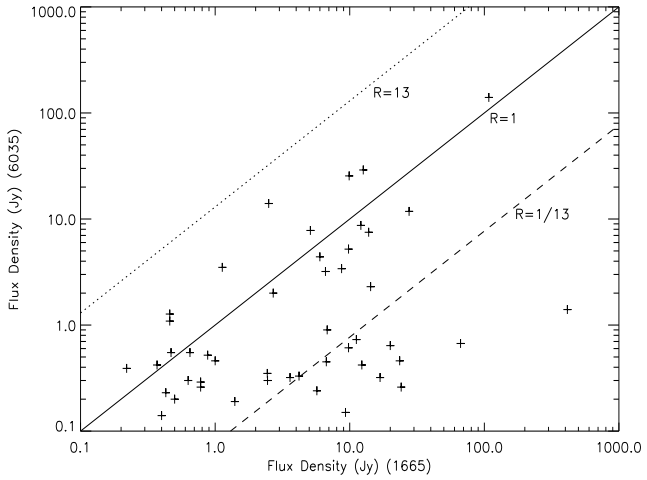

Figure 1. Flux density of 1665 MHz transition vs. Flux density of 6035 MHz transition. 47 sources having both transitions are represented with crosses.

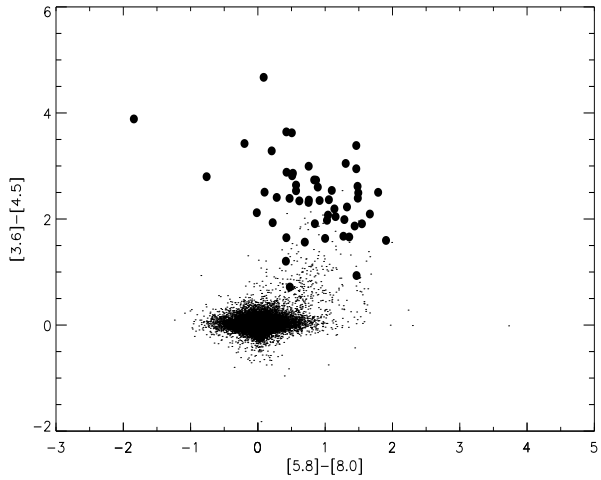

Figure 2. Color-color diagram constructed from GLIMPSE point source catalogue. The OH masers with GLIMPSE counterparts are represented with solid circles. Sources within 30′ radius of $l = 320.0^\circ, b = 0.0^\circ$ are represented with dots. Only sources for which there is flux density information for all four IRAC bands have been included in the plot, that is, 54 of 113 OH masers with a GLIMPSE point source within 2″ and 20018 of 101615 of the comparison sample.

4 DISCUSSION

4.1 GLIMPSE color

We have plotted color-color and color-magnitude diagrams for the GLIMPSE point sources associated with the interstellar OH masers which have better position accuracies with ATCA or VLA observations. For comparison, we choose the GLIMPSE sources within 30′ radius of $l = 320.0^\circ$, $b = 0.0^\circ$. The comparison sample from the GLIMPSE point source catalogue includes 101,615 sources and provides enough information to investigate the color and magnitude difference between maser-associated GLIMPSE sources and normal GLIMPSE sources. The interstellar OH masers are from C98 with ATCA observations and A2000 with VLA observations. The former sample includes 206 interstellar OH masers and the latter sample contains 91 interstellar OH masers. Then we associate the positions of these two samples taking 2″ as the separation criterion and obtain 266 interstellar OH masers. The positional accuracy of these 266 interstellar OH masers is about 0.4″. Among these 266 interstellar OH masers, 219 OH masers are in the GLIMPSE survey region ($|l| \leqslant 65^\circ$), and 113 OH masers are associated with GLIMPSE point sources within a 2″radius. The maser-associated GLIMPSE sources are obviously offset from the majority of the comparison sources in the color-color and color-magnitude diagrams and have much redder colors. The conclusion can be easily drawn from Fig. 2, which is a plot of the [5.8]-[8.0] versus [3.6]-[4.5] colors, showing that the maser-associated sources mostly lie above the vast majority of the comparison sources. This result is similar to the color-color diagram of methanol masers (see Figure 15 of Ellingsen 2006).

The sources associated with interstellar OH masers lie in a distinctive region of GLIMPSE color-color diagrams and occupy the same area as methanol masers. This result is interesting, but what can we derive from it? As discussed by Ellingsen (2006), polycyclic aromatic hydrocarbon (PAH) emission and silicate absorption lines can complicate the problem and affect some of IRAC bands (see Draine 2003 for a detailed discussion). But the actual influence of PAH emission and silicate absorption on the observed IRAC colors needs to be confirmed and measured by MIR spectroscopy.

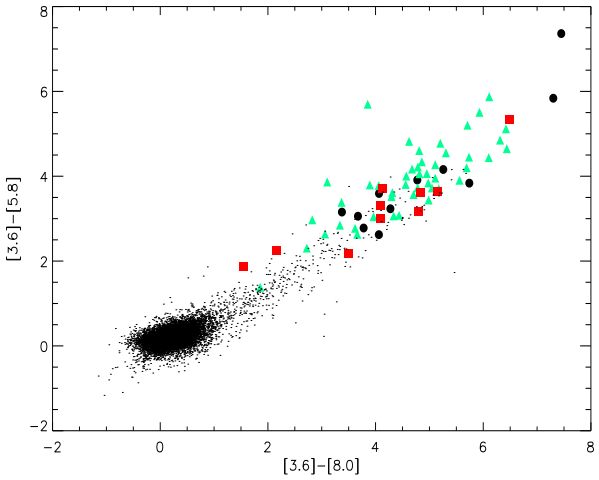

Figure 3. GLIMPSE [3.6]-[8.0] vs. [3.6]-[5.8] color-color diagram. The OH masers with associated GLIMPSE point sources are represented with solid circles if they don't have associated methanol multibeam (MMB) masers, as solid triangles if they have. The solid squares represent the methanol masers with associated GLIMPSE point sources but without associated OH masers, and these methanol masers are from Ellingsen (2006). Sources within 30′ radius of $l = 320.0°, b = 0.0°$ are represented with dots.

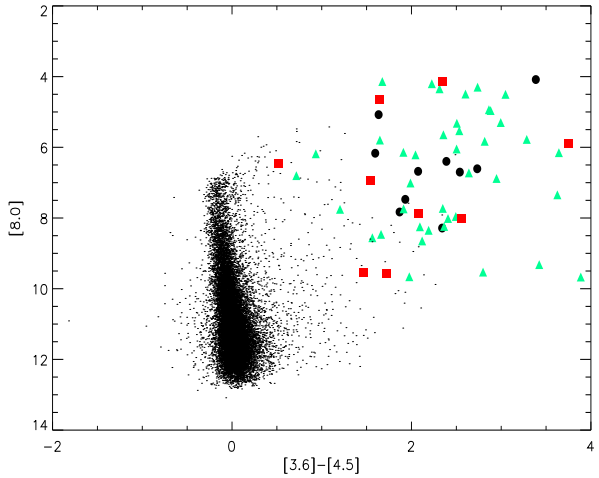

Figure 4. GLIMPSE [3.6]-[4.5] vs. 8.0 μm color-magnitude diagram. The OH masers with associated GLIMPSE point sources are represented with solid circles if they don't have associated methanol multibeam (MMB) masers, as solid triangles if they have. The solid squares represent the methanol masers with associated GLIMPSE point sources but without associated OH masers, and these methanol masers are from Ellingsen (2006). Sources within 30′ radius of $l = 320.0°, b = 0.0°$ are represented with dots.

For this reason the interpretation of GLIMPSE colors of maser-associated sources is uncertain to a large degree. Nevertheless, it is still meaningful to make the comparison between the GLIMPSE point sources with and without OH masers, because they all suffer the same effects and limitations with the same instrument.

The modeling of Whitney et al. (2003) shows that Class 0 objects lie in the same area in the GLIMPSE [5.8]-[8.0] versus [3.6]-[4.5] color-color diagram as the interstellar OH masers and the methanol masers. It is interesting to see whether or not OH masers trace the same evolutionary stage as methanol masers. The methanol multibeam (MMB) survey is a blind survey with longitudes from 186° to 20° and includes 707 6.7 GHz Class II methanol masers in total (Caswell et al. 2010; Green et al. 2010; Caswell et al. 2011; Green et al. 2012). We cross-match the positions of 707 MMB masers and 113 interstellar OH masers which are associated with GLIMPSE point sources within 2″. Finally we obtain 79 OH masers which are also associated with methanol masers and 25 OH masers which are not associated with methanol masers (solitary OH masers for short). Besides we collect 35 methanol masers without an associated OH maser (solitary methanol masers for short) from Table 1 of Ellingsen's (2006) paper. The sample of his paper is a statistically complete sample detected in the Mt.Pleasant survey (Ellingsen et al. 1996) and includes 56 methanol masers. Among the 35 solitary methanol masers, only 17 methanol masers have GLIMPSE counterparts. We construct color-color and color-magnitude diagrams for these three samples. Fig. 3 plots a [3.6]-[8.0] versus [3.6]-[5.8] color-color diagram, using different symbols for the three samples of maser-associated GLIMPSE sources. The comparison sources are also shown with dots. Fig. 3 shows that the colors of the solitary methanol masers tend to be little bluer than that of the solitary OH masers, but not obviously, and the OH masers with an associated methanol maser lie between them. Fig. 4 shows the [3.6]-[4.5] color and 8.0 μm magnitude diagram. There is no obvious difference among the solitary methanol masers, the OH masers with an associated methanol maser and the solitary OH masers. This result suggests that these two masers are possibly tracing closely evolutionary stage and cannot be clearly distinguished from the GLIMPSE color-color and color-magnitude diagrams, which is different from Figure 19 of Ellingsen (2006) which shows that methanol masers with associated OH masers are generally brighter at 8.0 μm than those without. Perhaps the data is not large enough to reveal the color and magnitude difference between the two species of masers. Thus it is still necessary and interesting to compare the MIR properties of the GLIMPSE sources associated with OH masers and methanol masers in a larger and more complete sample in order to investigate maser evolutionary sequence.

4.2 *WISE* colors

Since *WISE* has lower angular resolution than GLIMPSE, we take 6″ as the criterion to search for the *WISE* counterparts for 266 interstellar OH masers. Among 266 OH masers, 205 OH masers have *WISE* counterparts. After cross-matching them with 707 MMB masers, we obtain 32 OH masers without an associated methanol maser (solitary OH masers), which also lie in the MMB survey region. We get 139 OH masers which have associated methanol masers. We also search for the *WISE* counterparts for the 35 methanol masers without an associated OH maser (solitary methanol masers) from Table 1 of Ellingsen's paper (2006), and we find 23 *WISE* counterparts within 6″. For comparison, we select the *WISE* sources within 20′ radius of $l = 300°$, $b = 0°$. The comparison sample includes 7729 sources and has enough color and magnitude information

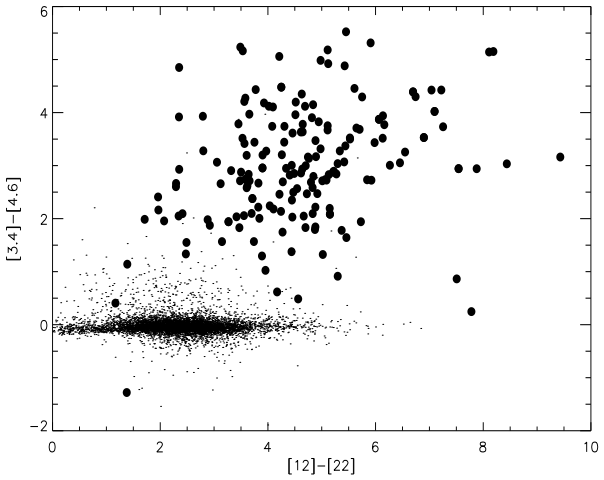

Figure 5. Color-color diagram constructed from *WISE* point source catalogue. The OH masers with *WISE* counterparts are represented with solid circles. Sources within 20′ radius of $l = 300°, b = 0°$ are represented with dots. Only sources for which there is flux density information for all four bands have been included in the plot, that is, 181 of 205 OH masers with a *WISE* point source within 6″ and 7728 of 7729 of the comparison sample.

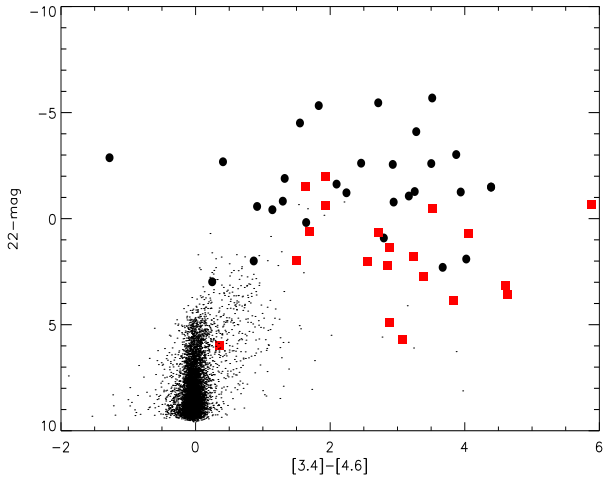

Figure 6. *WISE* [3.4]-[4.6] vs. 22 μm color-magnitude diagram. The OH masers with associated *WISE* point sources are represented with solid circles if they do not have associated methanol multibeam (MMB) masers. And the methanol masers with associated *WISE* point sources are represented with solid squares if they don't have associated OH masers. *WISE* point sources within 20′ radius of $l = 300°, b = 0°$ are represented with dots.

for detailed MIR environment study. Then we construct the color-color and color-magnitude diagrams for these four samples including comparison sample to investigate the MIR environment of masers. The maser-associated *WISE* sources are clearly offset from the vast majority of the comparison sources in most of the color-color and color-magnitude diagrams, and their colors are much redder. These features are the same as their GLIMPSE features. This can be clearly seen in Fig. 5, which plots the [12] - [22] versus [3.4] - [4.6] color-color diagram, showing the deviation between the maser-associated *WISE* sources and the comparison sources.

Fig. 6 plots the color-magnitude diagram of [3.4] - [4.6] color versus 22 μm magnitude, which shows that the solitary OH masers have a brighter MIR source counterpart at 22 μm, compared to the solitary methanol masers. We also plot the histograms of the four bands for the *WISE* sources associated with solitary OH masers and solitary methanol masers. We find that at 4.6, 12, 22 μm, there is a trend that the *WISE* sources associated with solitary OH masers are brighter than the *WISE* sources associated with solitary methanol masers, and it is most obvious at 22 μm band (shown in Fig. 7). This result may have a bias because the 22 μm magnitude depends on the distance. However, the *WISE* sources associated with these two kinds of masers all suffer from the same effect, and the obvious tendency could still illustrate some problems. The 22 μm band should trace the same dust emission components as the 24 μm band, which likely comes from very small grains (VSGs) out of thermal equilibrium, or a combination of emission from VSGs and from a larger grain population whose temperature is closer to 25 K (Anderson et al. 2012). The OH masers with the brighter 22 μm emission may trace a later evolutionary stage of the central star than the methanol masers because of the higher dust temperature. Cragg et al. (2002) found that the gas-phase molecular abundance is the key determinant of maser activity for both CH_3OH and OH masers. A

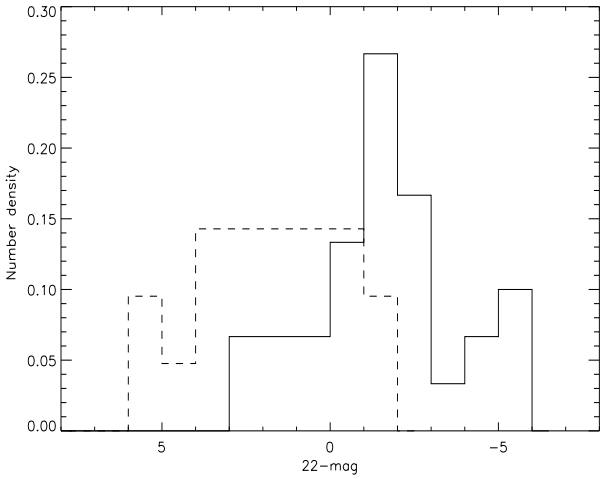

Figure 7. The distribution of 22 μm magnitude. The dashed curve shows the distribution of the methanol masers without associated OH masers, and the solid curve is that of the OH masers without associated methanol masers.

large CH_3OH column density can be easily reached in SFRs due to a high abundance of methanol ice on grain mantles (Dartois et al. 1999). OH abundance can be enhanced by the photodissociation or ion-molecule process after the H_2O molecules are injected into the gas phase. Charnley et al. (1992, 1995) predicted that a maximum of methanol abundance appears before a peak of OH abundance. If these models are confirmed by further chemical modeling, this would support the proposed evolutionary sequence mentioned above. Alternatively, the stellar mass range associated with OH masers may extend to higher masses than that for methanol masers as revealed by Ellingsen (2006).

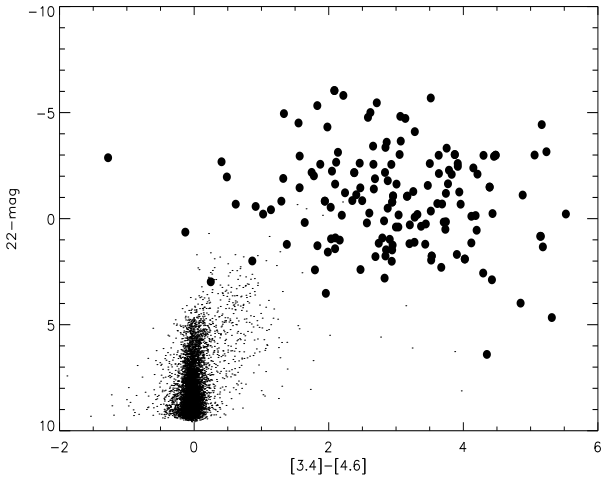

Figure 8. *WISE* [3.4]-[4.6] vs. 22 μm color-magnitude diagram for the OH masers same as Fig. 5. The OH masers with *WISE* counterparts are represented with solid circles. Sources within 20′ radius of $l = 300^\circ, b = 0^\circ$ are represented with dots.

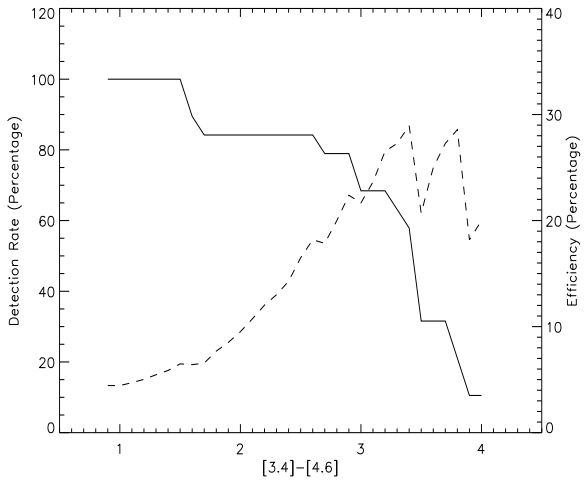

Figure 9. *WISE* [3.4]-[4.6] color vs. Detection Rate/Efficiency diagram (22 μm magnitude < 3). The Detection Rate is represented with the solid line. And the Efficiency is represented with the dashed line.

The distinctive color-color and color-magnitude properties of the *WISE* sources associated with OH masers provide an opportunity to create a *WISE*-selected target sample for future OH maser searches. Fig. 8 is the [3.4]-[4.6] vs. 22 μm color-magnitude diagram, showing that the majority (∼80%) of the *WISE* sources associated with known OH masers locate in a domain of $[3.4] - [4.6] > 2$ and 22 μm magnitude < 3, while nearly null sources in the comparison field locate in this domain. On the other hand, it is possible to estimate the detection rate and efficiency of an OH maser search targeted toward *WISE* point sources by comparing with one blind or untargeted OH maser survey. One untargeted survey with the Parkes by Caswell et al. (1980) had detected 19 interstellar OH masers in the region of $l = 330^\circ - 340^\circ$, $b = -0.3^\circ$ to 0.3° at a sensitivity of ∼0.1 Jy. For a search with a single dish, any targets that lie within half the FWHM beam could be searched only once in a single pointing. Considering the spatial coverage of the Parkes beam (∼10 ′ at 1.66 GHz), the actual targeted *WISE* sources could be deduced. Based on these, we plot the dependence of the detection rate and efficiency with the [3.4]-[4.6] color (under 22 μm magnitude < 3) in Figure 9, using the *WISE* sources and the OH maser data in the Caswell et al. (1980) surveyed region. From this figure, for the *WISE* sources satisfying the criteria of $[3.4] - [4.6] > 2$ and 22 μm magnitude < 3, 84% (16/19) of known OH masers in the blind survey would be expected to detect, this detection rate/percent is consistent with that (80%) shown in Fig. 8 for all known OH masers. Therefore, this also suggests that it is more reasonable to estimate a detection efficiency of OH maser searches using the criteria of $[3.4] - [4.6] > 2$ and 22 μm magnitude < 3, under which a detection efficiency of ∼10% would be achieved. We searched for the *WISE* All-sky Data Release and found about 7559 point sources satisfying the criteria. These *WISE* sources would provide a potential target sample for the further OH maser searches, especially with the newly-built 65 meter radio telescope in Shanghai. It should be noted that this new telescope has a similar beamsize to the Parkes dish. As a simple estimation, considering the beam coverage of the Shanghai 65 meter or Parkes telescope, the target pointing positions are reduced to 5209 towards these *WISE*-selected sources, thus ∼500 ground-state interstellar OH masers would be expected to detect. The expected total number of ground-state interstellar OH masers would be ∼600 in our Galaxy after considering that 84% of all OH masers would be detected from the above statistics.

4.3 Bubble-Like structures

The *Spitzer*-GLIMPSE images revealed a large number of full or partial ring-like structures, which were referred to as bubbles (Churchwell et al. 2006; Churchwell et al. 2007). Bubbles are a common phenomenon in the ISM. Most of them may be produced by newly formed massive stars and clusters, which excite PAHs in the swept up shell, and the PAHs are strong emitters at 8 μm in the photodissociation regions (PDRs) surrounding the HII region (Deharveng et al. 2010). Churchwell et al. (2006, 2007) (hereafter CH06, CH07) have catalogued about 600 ring structures traced mainly by 8.0 μm emission between Galactic longitudes -65° to 65° by inspecting the GLIMPSE I/II mosaic visually. Deharveng et al. (2010) studied a gallery of bubbles mainly from Churchwell et al. (2006), finding that 86% of their bubbles enclose HII regions. Good correlation of MIR bubbles with known HII regions or radio-continuum emission at 20 cm, and relatively low contamination from asymptotic giant brunch (AGB) star bubbles, supernova remnants (SNRs) and planetary nebulae (PNe) reported in the literature, indicates that bubbles are a good tracer of star formation activity (Churchwell et al. 2006; Deharveng et al. 2010). Deharveng et al. (2010) also concluded that more than a quarter of the bubbles may have triggered the formation of massive objects. The majority studies into triggered star formation by the expansion of bubbles take advantage of multiwavelength data sets (typically with near-, mid-, far-infrared, millimeter and radio wavelengths) to estimate the mass, age, and luminosity of

Table 6. Maser-associated bubbles.

Catalogue No.	l (deg)	b (deg)	R_{out} (arcmin)	Eccentricity	$\langle R \rangle$ (arcmin)	$\langle T \rangle$ (arcmin)	Morphology Flags	Name (OH)	Name (CH3OH)
N2	10.747	-0.468	8.31	0.56	6.95	1.23	B	G10.623-0.383	
N65	35.000	0.332	2.59	0.49	2.15	0.54	C	G35.024+0.350	
N68	35.654	-0.062	6.06	0.72	4.68	0.74	C,CC	G35.577-0.029	
S36	337.971	-0.474	3.56	0.66	2.73	0.69	C	G337.916-0.477	
S62	331.316	-0.359	2.50	0.58	2.02	0.45	B	G331.342-0.346	G331.342-0.346
S66	330.781	-0.414	7.42	0.69	5.63	1.37	B,CC,MB	G330.878-0.367	
								G330.878-0.367	
S110	316.809	-0.031	1.82	0.63	1.42	0.36	C,TP	G316.811-0.057	G316.811-0.057
S122	313.418	0.128	8.69	0.78	6.22	1.31	C	G313.469+0.190	G313.469+0.190
S169	301.122	-0.152	4.06	0.34	3.40	1.07	B	G301.136-0.226	G301.136-0.226
CN15	0.562	-0.843	1.03	0.73	0.71	0.27	B, BC	G0.546-0.852	
CN71	5.894	-0.463	6.17	0.38	5.45	0.96	B, FL, Y	G5.886-0.393	
								G5.885-0.392	
CN135	9.612	0.196	0.48	0.69	0.34	0.13	C, BC	G9.619+0.193	G09.619+0.193
								G9.620+0.194	
								G9.621+0.196	G09.621+0.196
CS1	359.965	-0.502	2.74	0.67	2.15	0.42	B, Y	G359.970-0.457	G359.970-0.457
CS43	354.715	0.297	0.51	0.70	0.38	0.11	C, Y	G354.724+0.300	G354.724+0.300
CS46	354.619	0.492	1.25	0.50	1.04	0.24	C, BC, Y	G354.615+0.472	G354.615+0.472
CS55	353.417	-0.375	1.34	0.91	0.78	0.15	B	G353.410-0.360	G353.410-0.360
CS73	352.174	0.297	6.80	0.62	5.52	1.02	B	G352.161+0.200	
CS106	350.327	0.096	1.02	0.75	0.74	0.18	B, CS	G350.329+0.100	

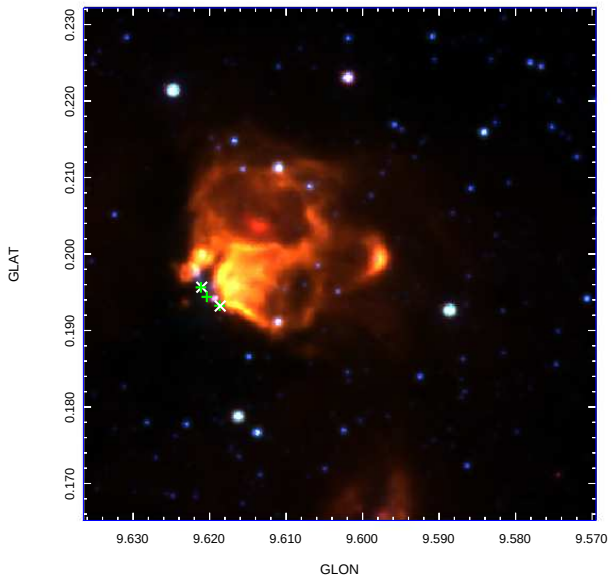

Figure 10. The three-color (4.5 μm: blue; 5.8 μm: green; 8.0 μm: red) image of the bubble CN135 from CH07 catalogue, with three OH masers (plus) located on the border of the bubble and two methanol masers (cross) sharing the same sites with their associated OH masers.

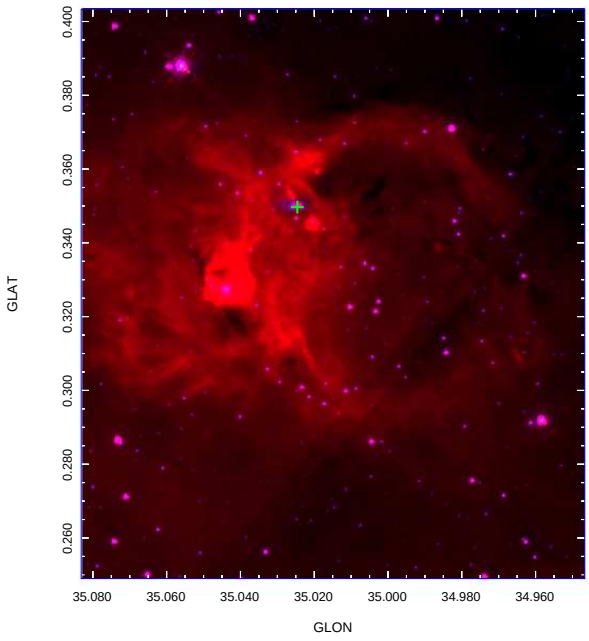

Figure 11. Same as Fig. 10, but for the bubble N65 from CH06 catalogue. Notably only one OH maser (plus) is located on the border of the bubble.

triggering and triggered sources, and compare the kinematic properties of the young stars with the surrounding ISM. The evidence of triggered star formation has thus been reported in several known HII regions and bubbles, e.g. Sh2-212 (Deharveng et al. 2008), W51a (Kang et al. 2009), RCW120 (Zavagno et al. 2010), S51 (Zhang et al. 2012), N4 (Li et al. 2013), and G52L (Li et al. 2013). Although these studies provide reasonable evidence of triggered star formation, they always conclude with uncertainties and open questions such as the uncertainties of the association between YSOs and the collected material (Kang et al. 2009) and the age uncertainties of stars in the condensation regions (Zavagno et al. 2010). Kendrew et al. (2012) took a statisti-

cal approach to investigate the association of bubbles with massive star formation and found a strong positional correlation of massive young stellar objects (MYSOs) and bubbles. However, it is yet not clear whether the expansion of bubbles could cause the following generation of stars. Interstellar OH masers trace the massive star formation, thus, the association study between interstellar OH masers and bubbles may obtain the indirect evidence supporting the triggered star formation by the expansion of bubbles.

We use the catalogue made by Churchwell et al. (2006, 2007) which contains 591 bubbles to study the association between bubbles and 219 interstellar OH masers mentioned above. Churchwell et al. (2006, 2007) measured the bubbles' parameters such as their semimajor (R_{out}) and semiminor (r_{out}) axes of the outer ellipse. We use $1.2R_{out}$ as the criterion to cross-match the OH maser positions and the bubble center positions. The criteria is larger than R_{out} because the definition of R_{out} is subjective. We find that 18 bubbles are associated with 22 OH masers. Among them, one bubble (CN135) is associated with three OH masers, and two bubbles (CN71, S66) are associated with two OH masers, respectively. These associations may be caused by merely geometric effects, but still need to be investigated. Here we assume all the masers are associated with bubbles. Then we cross-match these 22 OH masers with 707 MMB masers taking $2''$ criterion. The result is that ten methanol masers are associated with ten OH masers and nine bubbles. The basic information about 18 maser-associated bubbles and the names of the associated OH masers and methanol masers are also listed in Table 6.

The low association between bubbles and interstellar OH masers may be due to the maser sample we used. The 219 OH masers as described above are mainly from targeted surveys. Therefore, many bubbles may not have been searched for OH masers on the boarders. In addition, the low association may suggest that the young stars on the boarders of the majority of the bubbles are at an early stage and have not developed the physical conditions suitable for the pumping of OH masers. Besides, the result may simply imply that the majority of the bubbles have not yet triggered the star formation on the borders, or the triggered star formation is inefficient on the borders of bubbles.

We display the false color images of the bubbles (4.5 μm: blue; 5.8 μm: green; 8.0 μm: red) using the display program ds9[1] and point out the positions of OH masers and methanol masers in the bubble infrared images. As examples, Fig. 10 shows the three-color image of the bubble CN135. It shows that three OH masers are located on the border of the bubble and two methanol masers share the same sites with OH masers. Fig. 11 is the three-color image of the bubble N65. It only has one OH maser on the boarder of the bubble. The remaining sixteen bubbles have the same maser distribution as CN135 or N65, and many masers are associated with bright emission at 8.0 μm. The 6.7 GHz Class II methanol masers and interstellar OH masers are the tracers of massive star formation. This result confirms that the massive star formation is ongoing on the border of bubbles and the bubbles may trigger the massive star formation by their outward expansion.

[1] See http://hea-www.harvard.edu/RD/ds9/ref

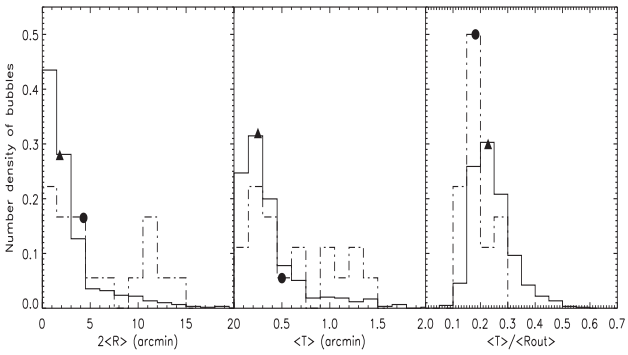

Figure 12. Observed distributions of average bubble angular diameters ($2\langle R\rangle$), average bubble thickness (angular measure $\langle T\rangle$) and bubble thickness relative to average outer radius ($\langle T\rangle/\langle R_{out}\rangle$). The dot dashed curves show the distributions of 18 maser-associated bubbles, and the solid curves are those of the 591 bubbles. The solid circles are the medians of 18 maser-associated bubbles, while the solid triangles are the medians of the 591 bubbles.

Beyond that, we study the properties of maser-associated bubbles. The left figure in Fig. 12 is the average angular diameter ($2\langle R\rangle$) distribution of 591 bubbles and 18 maser-associated bubbles. We can see from it that the average angular diameters of 18 maser-associated bubbles are slightly larger than that of 591 bubbles. The middle figure in Fig. 12 shows that there is a deviation of the average angular thickness ($\langle T\rangle$) between 18 maser-associated bubbles and 591 bubbles. From the right figure in Fig. 12, we can see that the ratio of average thickness to average outer radius ($\langle T\rangle/\langle R_{out}\rangle$) is smaller than 0.3 for 18 maser-associated bubbles. The $2\langle R\rangle$, $\langle T\rangle$, and $\langle T\rangle/\langle R_{out}\rangle$ medians for 591 bubbles and 18 maser-associated bubbles are labeled in Fig. 12. The $2\langle R\rangle$, and $\langle T\rangle$ medians of 18 maser-associated bubbles are $4.30'$ and $0.50'$, which are larger than $1.82'$ and $0.25'$ for 591 bubbles; The $\langle T\rangle/\langle R_{out}\rangle$ medians for 18 maser-associated bubbles and 591 bubbles are 0.182 and 0.228, respectively. Deharveng et al. (2010) suggest that the large size of bubbles correspond to an older age or evolution in the ISM with low densities. Churchwell et al. (2006) concluded that bubble shell thickness increases approximately linearly with shell radius. The measurements of larger average bubble angular diameter ($2\langle R\rangle$) and smaller thickness relative to average outer radius ($\langle T\rangle/\langle R_{out}\rangle$) of 18 maser-associated bubbles may suggest that the maser-associated bubbles are generally older than normal bubbles. However, these results may be simply due to the artifacts of small number statistics and need further studies.

5 SUMMARY

In this paper, we present the catalogues of all the detected interstellar OH masers of different transitions. We also used the GLIMPSE and *WISE* data to investigate the MIR environment of the interstellar OH masers, and explore the MIR environment differences between OH masers and methanol masers. Besides, we also studied the association between OH masers and bubbles.

For maser action, one must have the presence of OH

(from the dissociation of water vapor), intense IR radiation (to populate higher energy levels of OH which then cascade to lower states which are inverted by a combination of IR and collisions), and a long path where the velocity dispersion is small, so the maser intensity can rise to a level at which can be detected. An assumption is that the masers radiate have spherical shapes, so radiate in all directions. That is, the masers are not beamed in a certain direction.We found no obvious difference in the GLIMPSE color-color and color-magnitude diagrams for solitary OH masers, OH masers associated with methanol masers, and solitary methanol masers, and this result is different from previous studies (Ellingsen 2006). However, in the *WISE* color-magnitude diagram, the 22 μm magnitude of MIR counterparts of solitary OH masers is significantly brighter than that of solitary methanol masers. This may indicate that the stellar mass range associated with OH masers can extend to higher masses than that for methanol masers, or it may be because the OH masers trace a later evolutionary phase than methanol masers. For bubbles, 22 OH masers are associated with 18 bubbles. Among them, ten OH masers are also associated with Class II methanol masers. The OH masers and methanol masers are usually found on the border of the bubbles, suggesting there are ongoing star formation activities. This result is the indirect evidence of the triggered star formation by the expansion of bubbles.

ACKNOWLEDGMENTS

We thank the refree for the helpful comments and constructive suggestions. This work is based in part on observations made with the Spitzer Space Telescope, which is operated by the Jet Propulsion Laboratory, California Institute of Technology under a contract with National Aeronautics and Space Administration (NASA). This publication makes use of data products from the Wide-field Infrared Survey Explorer, which is a joint project of the University of California Institute of Technology, funded by NASA. We would like to thank the Key Laboratory of Radio Astronomy, Chinese Academy of Sciences. This work is partly supported by China Ministry of Science and Technology under State Key Development Program for Basic Research (2012CB821800), the National Natural Science Foundation of China (grants 10625314, 11073041, 11103006, 11121062, 11133008, and 11273043), the Knowledge Innovation Program of the Chinese Academy of Sciences (Grant No. KJCX1-YW-18), the Scientific Program of Shanghai Municipality (08DZ1160100), the CAS/SAFEA International Partnership Program for Creative Research Teams, the Strategic Priority Research Program "The Emergence of Cosmological Structures" of the Chinese Academy of Sciences, Grant No. XDB09000000, and the Shanghai Tian Ma Telescope Pre-research Funding.

REFERENCES

Anderson L. D., Zavagno A., Barlow M. J. et al., 2012, A&A, 537, 1
Argon A. L., Reid M. J., Karl M. Menten., 2000, ApJS, 129, 159, (A2000)
Bains I., Caswell J., Richards A. M. S. et al., 2008, IAU, 242, 2007
Baudry A., 1974, A&A, 33, 381
Baudry A., Desmurs J. F., Cohen R. J., 1997, A&A, 325, 255, (BD97)
Baudry A., Desmurs J. F., 2002, A&A, 394, 107, (BD2002)
Benjamin R. A. et al., 2003, PASP, 115, 953
Caswell J. L., Haynes R. F., Goss W. M., 1980, AuJPh, 33, 639
Caswell J. L., Haynes R. F., 1983, AuJPh, 36, 361
Caswell J. L., Haynes R. F., 1987, AuJPh, 40, 215
Caswell J. L., Vaile R. A., 1995, MNRAS, 273, 328, (CV95)
Caswell J. L., 1997, MNRAS, 289, 203
Caswell J. L., 1998, MNRAS, 297, 215, (C98)
Caswell J. L., 1999, MNRAS, 308, 683, (C99)
Caswell J. L., 2001, MNRAS, 326, 805, (C2001)
Caswell J. L., 2003, MNRAS, 341, 551, (C2003)
Caswell J. L., 2004, MNRAS, 352, 101, (C2004)
Caswell J. L., Kramer B. H., Sukom A. et al., 2010, MNRAS, 402, 2649
Caswell J. L., Fuller G. A., Green J. A. et al., 2010, MNRAS, 404, 1029
Caswell J. L., Fuller G. A., Green J. A. et al., 2011, MNRAS, 417, 1964
Charnley S. B., Tielens A. G. G. M., Millar T. J., 1992, ApJ, 399, L71
Charnley S. B., Kress M. E., Tielens A. G. G. M. et al., 1995, ApJ, 448, 232
Churchwell E., Povich M. S., Allen D. et al., 2006, ApJ, 649, 759
Churchwell E., Watson M. S., Povich M. S. et al., 2007, ApJ, 670, 428
Cohen R. J., Masheder M. R. W., Walker R. N. F., 1991, MNRAS, 250, 611, (CM91)
Cohen R. J., Masheder M. R. W., Caswell J. L., 1995, MNRAS, 274, 808, (CM95)
Cragg D. M., Sobolev A. M., Godfrey P. D., 2002, MNRAS, 331, 521
Dartois E., Schutte W., Geballe T. R. et al., 1999, A&A, 342, L32
Deharveng L., Lefloch B., Kurtz S. et al., 2008, A&A, 482, 585
Deharveng L., Schuller F., Anderson L. D. et al., 2010, A&A, 523, 6
Dodson R. G., Ellingsen S. P., 2002, MNRAS, 333, 307, (DE2002)
Draine B. T., 2003, ARA&A, 41, 241
Edris K. A., Fuller G. A., Cohen R. J., 2007, A&A, 465, 865, (EF2007)
Ellingsen S. P., von Bibra M. L., McCulloch P. M. et al., 1996, MNRAS, 280, 378
Ellingsen S. P., 2006, ApJ, 638, 241
Fish V. L., Sjouwerman L. O., 2007, ApJ, 668, 331
Forster J. R., Caswell J. L., 1999, A&A, 137, 43, (FC99)
Forster J. R., Caswell J. L., 1989, A&A, 213, 339
Gardner F. F., Martín-Pintado J., 1983, A&A, 121, 265
Green A. J., Frail D. A., Goss W. M. et al., 1997, AJ, 114, 2058
Green J. A., Caswell J. L., Fuller G. A. et al., 2010, MNRAS, 409, 913
Green J. A., Caswell J. L., Fuller G. A. et al., 2012, MNRAS, 420, 3108

Guilloteau S., 1982, A&A, 116, 101
Gundermann E. J., 1965, Ph.D. thesis, Harvard University
Harvey-Smith L., Cohen R. J., 2005, MNRAS, 356, 673, (SC2005)
Harvey-Smith L., Cohen R. J., 2007, IAU, 237, 2006
Hekkert P. L., Chapman J. M., 1996, A&AS, 119, 459
Kang M., Bieging J. H., Kulesa C. A. et al., 2009, ApJ, 701, 454
Kendrew S., Simpson R., Bressert E. et al., 2012, ApJ, 755, 71
Li J. Y., Jiang Z. B., Liu Y. et al., 2013, RAA, 13, 921
Li G. X., Wyrowski F., Menten K. et al., 2013, arXiv:1310.3267
Migenes V., Cruz-Vazquez L., Slysh V. I. et al., 2005, ASPC, 340, 361
Mu J. M., Esimbek J., Zhou J. J. et al., 2010, RAA, 10, 166
Palmer P., Goss W. M., Whiteoak J. B., 2004, MNRAS, 347, 1164, (PG2004)
Pavlakis K. G., Kylafis N. D., 1996, ApJ, 467, 309
Pavlakis K. G., Kylafis N. D., 2000, ApJ, 534, 770
Reid M. J., 2002, IAUS, 206, 506
Slysh V. I., Alakoz A. V., & Migenes V., 2010, MNRAS, 404, 1121
Smits D. P., 1994, MNRAS, 269, L11, (S94)
Smits D. P., 1997, MNRAS, 287, 253, (S97)
Smits D. P., 2003, MNRAS, 339, 1, (S2003)
Szymczak M., Kus A. J., Hrynek G., 2000, MNRAS, 312, 211, (SK2000)
Szymczak M., Gérard E., 2004, A&A, 414, 235, (SG2004)
Thacker D. L., Wilson W. J., Barrett A. H., 1970, ApJ, 161, L191
Turner B. E., Palmer P., Zuckerman B., 1970, ApJ, 160, L125
Weaver H., Williams R. W., Dieter N. H. et al., 1965, Natur, 208, 29
Whitney B. A., Wood K., Bjorkman J. E. et al., 2003, ApJ, 598, 1079
Wright E. L., Eisenhardt P. R. M., Mainzer A. K. et al., 2010, AJ, 140, 1868
Yen J. L., Zuckerman B., Palmer P. et al., 1969, ApJ, 156, L27
Zavagno A., Russeil D., Motte F. et al., 2010, A&A, 518, L81
Zhang C. P., Wang J. J., 2012, A&A, 544, A11
Zuckerman B., Palmer P., Penfield H. et al., 1968, ApJ, 153, L69

This paper has been typeset from a TEX/ LATEX file prepared by the author.

APPENDIX : ONLINE MATERIAL

Table 2. Catalogue of 18 cm Interstellar OH masers.

No.	Source name	RA(J2000) (h m s)	DEC(J2000) (^{o} ' ")	Freq. (MHz)	Vpeak (km s^{-1})	Vrange (km s^{-1})	Flux density (Jy)	Ref.	Other name
1	G126.715-0.822	01 23 33.17	+61 48 49.2	1665L	-12.06	-12.06,-8.64	>1.50	A2000	
1	G126.715-0.822	01 23 33.17	+61 48 49.2	1665R	-5.74		>0.50	A2000	
2	G133.715+1.215	02 25 40.59	+62 05 50.5	1665L	-39.29	-43.96,-37.59	>4.31	A2000	W3
2	G133.715+1.215	02 25 40.59	+62 05 50.5	1665R	-39.2		>0.75	A2000	W3
3	G133.946+1.064	02 27 03.70	+61 52 25.4	1612L	-43.15	-47.51,-42.3	>1.68	A2000	W3 OH
3	G133.946+1.064	02 27 03.70	+61 52 25.4	1612R	-42.17	-42.92,-41.48	>6.21	A2000	W3 OH
3	G133.946+1.064	02 27 03.70	+61 52 25.4	1665L	-46.29	-48.94,-41.93	>132.32	A2000	W3 OH
3	G133.946+1.064	02 27 03.70	+61 52 25.4	1665R	-45.02	-48.9,-40.02	>200.54	A2000	W3 OH
3	G133.946+1.064	02 27 03.70	+61 52 25.4	1667L	-44.43	-47.77,-43.31	>26.87	A2000	W3 OH
3	G133.946+1.064	02 27 03.70	+61 52 25.4	1667R	-42.17	-47.82,-45.04	>21.36	A2000	W3 OH
3	G133.946+1.064	02 27 03.70	+61 52 25.4	1720L	-45.56	-45.56,-43.5	>10.40	A2000	W3 OH
3	G133.946+1.064	02 27 03.70	+61 52 25.4	1720R	-44.33	-44.7,-42.72	>8.32	A2000	W3 OH
4	IRAS05137+3919	05 17 12.8	+39 22 05	1665R	-21.58	-24.5,-21.2	2.2	EF2007	
5	IRAS05274+3345	05 31 06.4	+33 47 27	1665R	-3.61	-5,0.6	1.34	EF2007	
5	IRAS05274+3345	05 31 06.4	+33 47 27	1667L	-4.93		0.14	EF2007	
5	IRAS05274+3345	05 31 06.4	+33 47 27	1612L	-3.87		0.13	EF2007	
6	IRAS05358+3543	05 39 13.0	+35 45 51	1665L	-10.88	-16.5,-8.5	2.82	EF2007	
6	IRAS05358+3543	05 39 13.0	+35 45 51	1667L	-10.53		0.93	EF2007	
7	IRAS05382+3547	05 41 12.9	+35 54 06	1665R	-26.83	-27,-26.5	0.5	EF2007	
8	G213.706-12.60	06 07 47.84	-06 22 56.7	1665L	11.48	8.29,11.48	>7.54	A2000	Mon R2
8	G213.706-12.60	06 07 47.84	-06 22 56.7	1665R	9.7	8.34,10.37	>19.01	A2000	Mon R2
8	G213.706-12.60	06 07 47.84	-06 22 56.7	1667L	10.75	8.39,10.75	>1.67	A2000	Mon R2
8	G213.706-12.60	06 07 47.84	-06 22 56.7	1667R	9.77	8.35,9.77	>2.14	A2000	Mon R2
9	IRAS06056+2131	06 08 52.4	+21 34 06	1665L	10.14	3,11	3.23	EF2007	
9	IRAS06056+2131	06 08 52.4	+21 34 06	1667R	9.44		0.22	EF2007	
9	IRAS06056+2131	06 08 52.4	+21 34 06	1720R	3.37		0.6	EF2007	
10	G188.946+0.886	06 08 53.33	+21 38 29.0	1665L	8.54		>0.60	A2000	S252
10	G188.946+0.886	06 08 53.33	+21 38 29.0	1665R	9.97	9.06,9.97	>0.72	A2000	S252
11	G196.454-1.677	06 14 37.07	+13 49 36.3	1665L	16.04	16.04,17.9	>8.73	A2000	S269
11	G196.454-1.677	06 14 37.07	+13 49 36.3	1665R	16.03	14.38,17.87	>1.53	A2000	S269
12	G232.621+0.996	07 32 09.82	-16 58 13.0	1665	21.8	20,25	1.7	C98	
13	G240.316+0.071	07 44 51.98	-24 07 42.4	1665	63	62,68	1.8	C98	
14	G263.250+0.514	08 48 47.80	-42 54 28.8	1665	15.3	6,16	0.42	C98	
15	G284.351-0.418	10 24 10.73	-57 52 33.3	1665	5.5	4,9	0.4	C98	
16	G285.263-0.050	10 31 29.87	-58 02 18.0	1665	6.5	2,15	24	C98	
17	G287.371+0.644	10 48 04.45	-58 27 01.2	1665	-4	-5,+1	0.6	C98	
18	G290.374+1.661	11 12 18.10	-58 46 20.3	1665	-23.3	-25,-12	1	C98	
19	G290.375+1.666	11 12 19.50	-58 46 04.9	1720	-20.5		0.6	C2004	
20	G291.610-0.529	11 15 02.59	-61 15 49.5	1665	18	16,22	6.3	C98	
21	G291.579-0.431	11 15 05.74	-61 09 40.7	1665	13	7,20	0.84	C98	
22	G294.511-1.621	11 35 32.22	-63 14 42.6	1665	-12.7	-14,-8	30	C98	
23	G297.660-0.973	12 04 08.99	-63 21 36.0	1665	27	22,30	1.05	C98	
24	G299.013+0.128	12 17 24.66	-62 29 03.7	1665	20.3	20,21	1.2	C98	
25	G300.504-0.176	12 30 03.49	-62 56 49.8	1665	22.4	3,24	1.1	C98	
26	G300.969+1.147	12 34 53.24	-61 39 40.3	1665	-40	-45,-34	8	C98	
26	G300.969+1.147	12 34 53.63	-61 39 40.0	1720	-42.2		0.35;0.35;0.35	C2004	
27	G301.136-0.226	12 35 35.07	-63 02 32.4	1665	-38.8	-64,-33	12	C98	
28	G305.208+0.206	13 11 13.78	-62 34 41.1	1665	-38	-44,-36	15.9	C98	
29	G305.200+0.019	13 11 16.90	-62 45 54.7	1665	-31.5	-40,-31	1.47	C98	
30	G305.362+0.150	13 12 35.87	-62 37 17.9	1665	-39.5	-42,-32	10.6	C98	
31	G305.799-0.245	13 16 43.32	-62 58 32.9	1665	-36.7	-37,-34	1.33	C98	
32	G306.322-0.334	13 21 23.00	-63 00 30.4	1665	-22.6	-25,-20	0.4	C99	
32	G306.322-0.334	13 21 23.07	-63 00 29.3	1720	-22.6		1.8;3.1;2.9	C2004	
33	G307.805-0.456	13 34 27.40	-62 55 13.8	1665	-16.5	-19,-13	7.5	C98	
34	G308.918+0.123	13 43 01.67	-62 08 51.9	1665	-54	-56,-50	56	C98	
35	G309.384-0.135	13 47 24.10	-62 18 12.5	1665	-52	-54,-49	0.23	C98	
36	G309.921+0.479	13 50 41.73	-61 35 09.8	1665	-60	-64,-58	27.6	C98	
37	G310.146+0.760	13 51 59.60	-61 15 39.6	1720	-55		1.2	C2004	
38	G311.643-0.380	14 06 38.76	-61 58 24.0	1665	38	15,50	6.8	C98	
39	G311.94+0.14	14 07 48.7	-61 23 22	1665	-41	-42,-40	0.4	C98	
40	G312.598+0.045	14 13 15.01	-61 16 53.6	1665	-62	-70,-59	3.6	C98	
41	G313.469+0.190	14 19 40.98	-60 51 47.1	1665	-10	-11,-6	1.57	C98	
42	G313.577+0.325	14 20 08.70	-60 41 59.9	1665	-47	-48,-46	0.78	C98	
43	G313.705-0.190	14 22 34.72	-61 08 27.4	1665	-44	-46,-41	0.88	C98	
44	G313.767-0.863	14 25 01.63	-61 44 58.1	1665	-53.5	-57,-49	5.5	C98	
45	G314.320+0.112	14 26 26.34	-60 38 31.6	1665	-74	-75,-44	0.61	C98	
46	G316.359-0.362	14 43 11.00	-60 17 15.3	1665	-0.5	-2,0	0.2	C98	
47	G316.412-0.308	14 43 23.34	-60 13 00.0	1665	-2	-9,-1	0.32	C98	
48	G316.640-0.087	14 44 18.35	-59 55 11.3	1665	-22	-35,-15	2.64	C98	
49	G316.763-0.012	14 44 56.34	-59 48 00.8	1665	-40	-41,-35	1.4	C98	
50	G316.811-0.057	14 45 26.34	-59 49 15.4	1665	-44	-45,-38	30	C98	
51	G317.429-0.561	14 51 37.62	-60 00 20.2	1665	25	22,27	3.87	C98	
52	G318.050+0.087	14 53 42.69	-59 08 56.2	1665	-53	-55,-48	10.8	C98	
53	G318.044-1.405	14 59 08.74	-60 28 25.7	1665	45	35,46	0.36	C98	
54	G318.948-0.196	15 00 55.36	-58 58 52.8	1665	-35.5	-42,-30	29.4	C98	
55	G319.398-0.012	15 03 17.41	-58 36 12.2	1665	-8.5	-11,-8	[0.75x1667]	C98	
56	G319.836-0.196	15 06 54.57	-58 32 57.1	1665	-10.5	-12,-6	0.56	C98	
57	G320.120-0.440	15 09 43.85	-58 37 05.8	1665	-55.5	-58,-54	0.7	C98	

58	G320.232-0.284	15 09 51.96	-58 25 38.3	1665	-67.5	-70,-59	6.5	C98
59	G321.030-0.485	15 15 51.67	-58 11 18.0	1665	-67	-70,-55	0.52	C98
60	G321.148-0.529	15 16 48.39	-58 09 50.2	1665	-63	-65,-60	1.7	C98
61	G322.158+0.636	15 18 34.62	-56 38 25.6	1665	-61	-65,-60	0.68	C98
62	G323.459-0.079	15 29 19.23	-56 31 22.0	1720	-68.5		0.35	C2004
62	G323.459-0.079	15 29 19.35	-56 31 22.3	1612	-70.8		0.96	C99
62	G323.459-0.079	15 29 19.36	-56 31 21.4	1665	-69	-72,-64	8.6	C99
63	G323.740-0.263	15 31 45.49	-56 30 50.7	1665	-46	-72,-39	1.2	C98
64	G324.200+0.121	15 32 52.92	-55 56 07.5	1665	-91.5	-94,-83	13.3	C98
65	G324.716+0.342	15 34 57.42	-55 27 24.0	1665	-54	-55,-49	0.43	C98
66	G326.670+0.554	15 44 57.21	-54 07 12.7	1665	-40.8	-41,-40	0.6	C98
67	G327.120+0.511	15 47 32.82	-53 52 39.4	1665	-80.5	-89,-80	6.5	C98
68	G326.77-0.26	15 48 56.5	-54 41 50	1665	-58	-59,-57	2.5	C98
69	G327.402+0.444	15 49 19.68	-53 45 14.3	1665	-77	-83,-76	2.4	C98
70	G327.291-0.578	15 53 07.78	-54 37 06.8	1665	-54.5	-72,-40	15.7	C98
71	G328.307+0.430	15 54 06.48	-53 11 40.3	1665	-92.8	-94,-90	14.4	C98
72	G328.809+0.633	15 55 48.49	-52 43 05.9	1720	-43.2		10	C2004
72	G328.809+0.633	15 55 48.55	-52 43 05.6	1665	-43.5	-50,-35	69.3	C99
73	G328.237-0.547	15 57 58.26	-53 59 22.5	1665	-41	-47,-30	5.7	C98
74	G328.254-0.532	15 57 59.80	-53 57 59.6	1665	-37	-54,-35	14.4	C98
75	G329.031-0.198	16 00 30.32	-53 12 27.8	1665	-45.5	-48,-45	1	C98
76	G329.029-0.200	16 00 30.38	-53 12 35.5	1665	-38.5	-40,-37	3.3	C98
77	G329.029-0.205	16 00 31.79	-53 12 49.8	1665	-38.5	-42,-36	9.1	C98
78	G329.339+0.148	16 00 33.14	-52 44 40.3	1720	-106.9		0.9;0.9	C2004
79	G329.066-0.308	16 01 09.94	-53 16 02.9	1665	-44	-45,-42	2.45	C98
80	G329.183-0.314	16 01 47.02	-53 11 43.7	1665	-53	-55,-47	3.8	C98
81	G329.426-0.158	16 02 19.02	-52 55 07.0	1720	-79		2.5;3.5;3.4	C2004
82	G329.405-0.459	16 03 32.15	-53 09 31.0	1665	-69.5	-76,-67	9.3	C98
83	G332.295+2.280	16 05 41.72	-49 11 30.5	1665	-20	-42,+6	0.86	C98
84	G330.953-0.182	16 09 52.02	-51 54 51.7	1720	-86		0.8	C2004
84	G330.953-0.182	16 09 52.43	-51 54 54.0	1665	-85.5	-95,-80	23.5	C98
85	G330.878-0.367	16 10 19.88	-52 06 07.1	1612	-62.9		0.31	C99
85	G330.878-0.367	16 10 20.01	-52 06 07.7	1665	-61.8	-72,-60	333	C99
86	G331.132-0.244	16 10 59.72	-51 50 22.7	1665	-88.5	-94,-88	13.3	C98
87	G331.278-0.188	16 11 26.57	-51 41 56.5	1665	-86.8	-92,-78	8.9	C98
88	G331.542-0.066	16 12 09.05	-51 25 47.2	1665	-86.5	-87,-83	5.5	C98
89	G331.512-0.103	16 12 09.88	-51 28 37.2	1612	-87	-90,-85	200	C99
89	G331.512-0.103	16 12 10.12	-51 28 37.7	1665	-91	-94,-85	22.7	C99
90	G331.442-0.186	16 12 12.41	-51 35 09.5	1665	-83	-84,-82	0.8	C98
91	G331.342-0.346	16 12 26.46	-51 46 16.3	1665	-66.5	-68,-64	5	C98
92	G331.556-0.121	16 12 27.19	-51 27 38.1	1665	-100	-103,-96	0.96	C98
93	G332.352-0.117	16 16 07.16	-50 54 30.4	1665	-44	-45,-42	0.77	C98
94	G333.315+0.105	16 19 29.00	-50 04 41.2	1665	-46	-47,-45	0.66	C98
95	G333.234-0.060	16 19 50.88	-50 15 10.8	1612	-91.2	-94,-82	1.7	C99
95	G333.234-0.060	16 19 50.90	-50 15 10.0	1665	-84	-94,-82	4.2	C99
96	G332.726-0.621	16 20 03.02	-51 00 32.1	1665	-46	-50,-44	0.73	C98
97	G333.387+0.032	16 20 07.58	-50 04 47.4	1665	-74	-75,-73	0.5	C98
98	G332.824-0.548	16 20 10.23	-50 53 18.1	1665	-54	-55,-53	1.77	C98
99	G333.135-0.431	16 21 02.97	-50 35 10.1	1665	-51	-56,-47	40	C98
100	G333.466-0.164	16 21 20.19	-50 09 48.2	1665	-43.5	-48,-36	3.4	C98
101	G333.608-0.215	16 22 11.04	-50 05 56.3	1612	-51.8	-56,50	1.8	C99
101	G333.608-0.215	16 22 11.06	-50 05 56.3	1665	-51	-57,-46	11	C99
102	G335.060-0.427	16 29 23.13	-49 12 26.9	1665	-41	-44,-40	1.4	C98
103	G335.789+0.174	16 29 47.37	-48 15 51.1	1665	-53	-55,-45	0.45	C98
104	G335.556-0.307	16 30 56.00	-48 45 51.0	1665	-113.3	-114,-113	0.08	C98
105	G335.585-0.285	16 30 57.33	-48 43 39.9	1665	-48	-49,-39	2.3	C98
106	G335.585-0.289	16 30 58.63	-48 43 50.8	1665	-53.5	-60,-49	2.2	C98
107	G336.358-0.137	16 33 29.16	-48 03 43.7	1665	-82	-84,-80	0.63	C98
108	G336.822+0.028	16 34 38.26	-47 36 33.0	1665	-75	-79,-74	0.47	C98
108	G336.822+0.028	16 34 38.37	-47 36 33.4	1720	-76		0.14	C2004
109	G336.864+0.005	16 34 54.39	-47 35 37.2	1665	-88	-90,-86	1.25	C98
110	G336.018-0.827	16 35 09.35	-48 46 47.1	1665	-42	-44,-40	0.9	C98
111	G336.994-0.027	16 35 33.88	-47 31 11.0	1720	-126		0.3	C2004
111	G336.994-0.027	16 35 33.95	-47 31 11.4	1665	-121	-125,-114	1.6	C98
112	G336.941-0.156	16 35 55.13	-47 38 45.3	1720	-69		0.6	C2004
112	G336.941-0.156	16 35 55.22	-47 38 45.7	1665	-68	-70,-65	0.46	C98
113	G336.984-0.183	16 36 12.46	-47 37 55.0	1665	-80.5	-82,-76	0.43	C98
114	G337.258-0.101	16 36 56.36	-47 22 26.8	1665	-70	-72,-68	0.98	C98
115	G338.280+0.542	16 38 09.05	-46 11 03.1	1665	-61	-63,-60	2.3	C98
116	G337.613-0.060	16 38 09.50	-47 04 59.8	1665	-42	-45,-39	1.5	C98
116	G337.613-0.060	16 38 09.50	-47 04 59.5	1720	-40.5		0.44	C2004
117	G337.707-0.051	16 38 29.55	-47 00 27.0	1665L	-49.26	-54.1,-48.68	>15.35	A2000
117	G337.707-0.051	16 38 29.55	-47 00 27.0	1665R	-50.85	-52.22,-49.46	>9.27	A2000
117	G337.707-0.051	16 38 29.55	-47 00 27.0	1667L	-49.27	-51.17,-49.27	>5.51	A2000
117	G337.707-0.051	16 38 29.55	-47 00 27.0	1667R	-49.83	-51.35,-49.83	>4.20	A2000
118	G337.705-0.053	16 38 29.68	-47 00 35.2	1665	-49	-55,-48	24.7	C98
119	G337.997+0.136	16 38 48.48	-46 39 57.6	1665	-35.5	-41,-32	7.7	C98
120	G337.405-0.402	16 38 50.57	-47 27 59.3	1665	-38	-58,-33	66.6	C98
121	G338.075+0.012	16 39 39.05	-46 41 28.0	1665	-47	-53,-44	2.44	C98
121	G338.075+0.012	16 39 39.16	-46 41 27.2	1720	-53		0.35;0.16	C2004
122	G338.472+0.289	16 39 58.88	-46 12 35.7	1665	-32	-33,-31	3.8	C98
123	G338.925+0.557	16 40 33.54	-45 41 35.9	1612	-62.9	-64,-60	23	C99
123	G338.925+0.557	16 40 33.57	-45 41 37.2	1665	-61	-65,-57	16.8	C99
123	G338.925+0.557	16 40 33.57	-45 41 37.2	1720	-61		0.8; <0.15	C2004
124	G337.920-0.456	16 41 06.07	-47 07 02.4	1665	-39.5	-40,-39	2.06	C98

125	G337.916-0.477	16 41 10.43	-47 08 03.1	1665	-52	-54,-31	21	C98	
126	G338.461-0.245	16 42 15.53	-46 34 18.7	1665	-56	-61,-55	3.3	C98	
127	G338.681-0.084	16 42 23.99	-46 17 59.4	1665	-22	-23,-19	4.8	C98	
128	G338.875-0.084	16 43 08.23	-46 09 12.8	1665	-36	-41,-33	2	C98	
129	G339.282+0.136	16 43 43.12	-45 42 08.4	1665	-72	-74,-67	0.88	C98	
130	G339.053-0.315	16 44 49.16	-46 10 14.4	1665	-111	-112,-109	0.37	C98	
131	G339.622-0.121	16 46 06.03	-45 36 43.7	1665	-37.3	-41,-30	20	C99	
131	G339.622-0.121	16 46 06.03	-45 36 43.9	1720	-37.3		0.4	C2004	
132	G340.054-0.244	16 48 13.88	-45 21 45.1	1665	-53.6	-59,-47	26	C98	
133	G340.785-0.096	16 50 14.81	-44 42 26.9	1665	-101	-108,-88	6	C99	
133	G340.785-0.096	16 50 14.81	-44 42 26.8	1720	-101		1.2	C2004	
133	G340.785-0.095	16 50 14.85	-44 42 23.3	1667L	-102.27	-102.65,-100.78	>2.94	A2000	
133	G340.785-0.095	16 50 14.85	-44 42 23.3	1667R	-101.79	-101.79,-101.57	>4.14	A2000	
134	G339.682-1.207	16 51 06.21	-46 15 57.8	1665	-23	-29,-22	2.3	C98	
135	G341.276+0.062	16 51 19.43	-44 13 44.5	1665	-73	-75,-72	0.43	C98	
136	G339.884-1.259	16 52 04.61	-46 08 34.1	1720	-34.8		1.9;3.3;10;10;12	C2004	
136	G339.884-1.259	16 52 04.67	-46 08 34.7	1665	-35	-40,-26	9.9	C98	
137	G341.218-0.212	16 52 17.84	-44 26 52.5	1665	-37.3	-42,-35	4.5	C98	
138	G345.010+1.792	16 56 47.58	-40 14 25.2	1665	-22.5	-31,-15	12.1	C98	
138	G345.011+1.792	16 56 47.61	-40 14 24.3	1667L	-20.01	-21.29,-17.98	>1.30	A2000	
138	G345.011+1.792	16 56 47.61	-40 14 24.3	1667R	-19.69		>1.71	A2000	
139	G345.118+1.592	16 57 57.96	-40 16 49.9	1720	-17		6.2	C2004	
140	G343.127-0.063	16 58 17.19	-42 52 08.4	1665	-31.5	-41,-29	55	C98	
141	G345.494+1.469	16 59 41.61	-40 03 43.3	1665	-12.7	-22,-7	3.8	C98	
142	G345.498+1.467	16 59 42.81	-40 03 36.2	1665	-15.5	-17,-13	4.6	C98	
143	G345.497+1.462	16 59 44.07	-40 03 51.9	1720	-20.5		4.9	C2004	
144	G343.930+0.125	17 00 10.92	-42 07 18.7	1665	11.9	10,14	1.13	C98	
145	G344.419+0.044	17 02 08.67	-41 47 08.6	1665	-65	-66,-64	0.5	C98	
146	G344.582-0.024	17 02 57.75	-41 41 53.4	1665	-2.3	-11,+2	29	C98	
146	G344.581-0.022	17 02 57.76	-41 41 51.6	1667L	-3.62	-10.25,0.7	>7.32	A2000	
146	G344.581-0.022	17 02 57.76	-41 41 51.6	1667R	-5.61	-9.63,-2.29	>3.91	A2000	
147	G344.227-0.569	17 04 07.81	-42 18 40.2	1665	-30.5	-32,-23	1.6	C98	
147	G344.227-0.568	17 04 07.81	-42 18 38.4	1667L	-29.88		>2.28	A2000	
147	G344.227-0.568	17 04 07.81	-42 18 38.4	1667R	-31.19	-31.19,-30.67	>6.87	A2000	
148	G345.504+0.348	17 04 22.87	-40 44 22.9	1665	-19.5	-26,-12	9.8	C98	
148	G345.505+0.347	17 04 22.98	-40 44 23.3	1667L	-19.73	-22.37,-12.74	>5.11	A2000	
148	G345.505+0.347	17 04 22.98	-40 44 23.3	1667R	-12.69	-22.37,-12.69	>4.87	A2000	
149	G345.488+0.313	17 04 28.13	-40 46 25.5	1665L	-22.81		>0.73	A2000	
150	G345.003-0.224	17 05 11.24	-41 29 07.5	1720	-27		20	C2004	
150	G345.003-0.224	17 05 11.25	-41 29 06.0	1667L	-27.73		>0.68	A2000	
150	G345.003-0.224	17 05 11.25	-41 29 06.0	1667R	-30.76	-30.76,-25.69	>3.47	A2000	
150	G345.003-0.224	17 05 11.26	-41 29 06.7	1665	-27	-32,-22	2.7	C99	
151	G345.437-0.074	17 05 56.59	-41 02 55.6	1665	-24.3	-35,-20	1.65	C98	
152	G345.698-0.090	17 06 50.57	-40 51 02.2	1612	-7.4	-9,-4	4.9	C99	
152	G345.698-0.090	17 06 50.62	-40 50 59.4	1665	-6	-9,-2	8.7	C99	
152	G345.699-0.090	17 06 50.64	-40 50 58.3	1667L	-6.15	-10.59,-5.14	>4.38	A2000	
152	G345.699-0.090	17 06 50.64	-40 50 58.3	1667R	-6.45	-8.27,-5.79	>12.78	A2000	
153	G346.481+0.132	17 08 22.76	-40 05 25.8	1665	-8	-9,-7	0.85	C98	
154	G345.407-0.952	17 09 35.45	-41 35 57.3	1665	-17.6	-19,-17	0.78	C98	
155	G347.628+0.148	17 11 50.99	-39 09 29.0	1612	-96.6	-98,-96	1.9	C99	
155	G347.628+0.148	17 11 51.02	-39 09 29.3	1665	-94.3	-99,-92	9.8	C99	
156	G347.870+0.014	17 13 08.80	-39 02 29.5	1665	-33	-34,-30	2.6	C98	
157	G348.89+0.10	17 15 50.13	-38 10 12.0	1665	-73.19	-73.74,-72.65	>2.40	FC99	
158	G348.884+0.096	17 15 50.15	-38 10 12.5	1665	-73.2	-76,-71	2.4	C98	
159	G349.092+0.106	17 16 24.59	-37 59 45.5	1665	-80	-91,-79	3.1	C98	
160	G349.067-0.017	17 16 50.74	-38 05 14.4	1665	15	14,16	2	C98	
161	G348.89-0.18	17 17 00.21	-38 19 28.8	1665	8.84	5.55,9.94	>1.20	FC99	
162	G348.892-0.180	17 17 00.21	-38 19 27.9	1665	9.5	3,11	1.29	C98	
163	G350.015+0.433	17 17 45.44	-37 03 12.9	1665	-33	-35,-32	0.81	C98	
164	G348.579-0.920	17 19 10.56	-39 00 24.5	1665	-27	-28,-26	1.4	C98	
165	G348.550-0.979	17 19 20.39	-39 03 51.8	1665	-19.7	-22,-10	6.8	C99	
165	G348.550-0.979	17 19 20.40	-39 03 51.5	1720	-19.7		2.6	C2004	
166	G350.11+0.09	17 19 24.72	-37 10 21.5	1665	-71.1	-76.04,-67.26	>31.80	FC99	
167	G350.113+0.095	17 19 25.58	-37 10 04.5	1665	-71	-77,-65	24.1	C98	
168	G351.160+0.697	17 19 57.35	-35 57 52.4	1665	-8.5	-16,+1	41.6	C98	
168	G351.161+0.697	17 19 57.41	-35 57 52.0	1667L	-12.59	-15.29,-4.49	>96.65	A2000	NGC 6334 B
168	G351.161+0.697	17 19 57.41	-35 57 52.0	1667R	-9.64	-15.23,-6.7	>78.82	A2000	NGC 6334 B
169	G348.698-1.027	17 19 58.91	-38 58 14.1	1665	-15.4	-18,-15	0.65	C98	
170	G350.329+0.100	17 20 01.61	-36 59 15.6	1665	-64	-65,-63	0.32	C98	
171	G348.703-1.043	17 20 03.96	-38 58 31.3	1665	-16.9	-18,-11	0.22	C98	
172	G348.727-1.037	17 20 06.55	-38 57 08.2	1665	-9.2	-12,-2	1.25	C98	
173	G348.70-1.04	17 20 06.69	-38 57 14.6	1665	-11.65	-11.65,-10.55	>0.70	FC99	
174	G351.232+0.682	17 20 13.29	-35 54 51.9	1667L	-12.6	-12.6,-9.01	>2.41	A2000	NGC 6334
174	G351.232+0.682	17 20 13.29	-35 54 51.9	1667R	-9.65	-14.14,-7.39	>1.89	A2000	NGC 6334
175	G351.417+0.645	17 20 53.37	-35 47 02.0	1720	-10.2		22;70.1	C2004	
175	G351.417+0.645	17 20 53.39	-35 47 01.8	1665	-9.1	-13,-6	108	C99	
175	G351.416+0.646	17 20 53.44	-35 47 01.6	1667L	-9.25	-12.46,-7.15	>48.58	A2000	NGC 6334 F
175	G351.416+0.646	17 20 53.44	-35 47 01.6	1667R	-11.11	-12.33,-6.61	>56.58	A2000	NGC 6334 F
176	G350.686-0.491	17 23 28.62	-37 01 48.5	1720	-15		0.6	C2004	
176	G350.686-0.491	17 23 28.68	-37 01 48.1	1665	-14.5	-15,-13	0.46	C98	
177	G352.161+0.200	17 24 46.28	-35 25 20.2	1665	-42.2	-43,-41	1.77	C98	
178	G350.011-1.342	17 25 06.50	-38 04 00.7	1665	-18.3	-27,-17	5.6	C98	
178	G350.011-1.341	17 25 06.51	-38 04 00.0	1667L	-23.74	-23.74,-19.32	>2.25	A2000	
178	G350.011-1.341	17 25 06.51	-38 04 00.0	1667R	-23.75	-23.75,-19.37	>2.58	A2000	
179	G351.581-0.353	17 25 25.25	-36 12 45.1	1665	-97.6	-101,-89	5.1	C98	

180	G351.775-0.536	17 26 42.44	-36 09 20.0	1720	-2		2.9;6.2	C2004	
180	G351.775-0.536	17 26 42.53	-36 09 18.1	1612	1.3	-5,+5	1.5	C99	
180	G351.775-0.538	17 26 42.55	-36 09 17.6	1667L	-6.96	-26.12,2.31	>59.11	A2000	
180	G351.775-0.538	17 26 42.55	-36 09 17.6	1667R	-8.81	-27.43,2.24	>6.74	A2000	
180	G351.775-0.536	17 26 42.56	-36 09 17.6	1665	-2	-29,+8	414	C99	
181	G353.464+0.562	17 26 51.56	-34 08 24.8	1665	-45	-46,-43	1.3	C98	
182	G352.517-0.155	17 27 11.34	-35 19 32.2	1665	-50.6	-56,-43	3	C98	
183	G354.615+0.472	17 30 17.07	-33 13 54.6	1665	-15.4	-34,-13	4	C99	
183	G354.615+0.472	17 30 17.11	-33 13 54.1	1612	-15		0.24	C99	
184	G353.410-0.360	17 30 26.20	-34 41 45.5	1665	-19.7	-21,-18	12.6	C99	
184	G353.410-0.360	17 30 26.20	-34 41 45.7	1720	-19.7		11	C2004	
185	G352.630-1.067	17 31 13.91	-35 44 08.4	1665	0	-2,+1	0.22	C98	
186	G354.724+0.300	17 31 15.52	-33 14 05.3	1665	95	90,97	0.7	C98	
187	G355.344+0.147	17 33 29.05	-32 47 58.2	1665	19	14,21	14.3	C98	
188	G356.662-0.264	17 38 29.22	-31 54 40.6	1665	-54.2	-55,-53	1.57	C98	
189	G358.235+0.116	17 40 54.16	-30 22 38.1	1667L	-26.4	-32.71,-24.65	>3.68	A2000	
189	G358.235+0.116	17 40 54.16	-30 22 38.1	1667R	-32.16	-32.4,-21.22	>0.76	A2000	
189	G358.23+0.11	17 40 54.23	-30 22 39.0	1665	-27.19	-29.94,-22.81	>2.80	FC99	
190	G357.968-0.163	17 41 20.36	-30 45 05.5	1665	-6.3	-10,-4	0.35	C98	
191	G359.137+0.032	17 43 25.62	-29 39 17.3	1665	-1	-7,0	11.2	C98	
192	G358.387-0.482	17 43 37.72	-30 33 48.3	1665	-6.3	-7,-5	0.73	C98	
193	G359.436-0.103	17 44 40.54	-29 28 15.1	1665	-52	-53,-50	4.05	C98	
194	G359.615-0.243	17 45 39.07	-29 23 29.1	1665	22.5	19,26	3.07	C98	
195	G0.496+0.188	17 46 04.03	-28 24 52.6	1665	-5.5	-7,-5	0.25	C98	
196	G0.376+0.040	17 46 21.38	-28 35 39.2	1665	36	28,40	4.7	C98	
197	G0.678-0.027	17 47 19.90	-28 22 16.8	1612L	64.77	64.46,64.77	>0.60	A2000	Sgr B2
197	G0.678-0.027	17 47 19.90	-28 22 16.8	1665L	70.11	69.27,73.57	>6.95	A2000	Sgr B2
197	G0.678-0.027	17 47 19.90	-28 22 16.8	1665R	62.02	62.02,71.1	>2.69	A2000	Sgr B2
198	G0.672-0.031	17 47 20.03	-28 22 41.5	1665L	54.41		>3.88	A2000	Sgr B2N
198	G0.672-0.031	17 47 20.03	-28 22 41.5	1665R	49.78	46.42,55.62	>4.28	A2000	Sgr B2N
198	G0.672-0.031	17 47 20.03	-28 22 41.5	1667L	48.02	47.39,48.02	>1.62	A2000	Sgr B2N
198	G0.672-0.031	17 47 20.03	-28 22 41.5	1667R	47.38	46.21,49.89	>2.52	A2000	Sgr B2N
199	G0.666-0.035	17 47 20.10	-28 23 10.5	1720	61.2		2	C2004	
199	G0.666-0.035	17 47 20.12	-28 23 06.2	1665	61	48,62	28.6	C98	
199	G0.666-0.034	17 47 20.13	-28 23 06.1	1612L	66.83	55.93,67.4	>1.36	A2000	Sgr B2M
199	G0.666-0.034	17 47 20.13	-28 23 06.1	1612R	59.26	54.58,66.45	>1.41	A2000	Sgr B2M
199	G0.666-0.034	17 47 20.13	-28 23 06.1	1667L	58.65	50.46,67.31	>2.13	A2000	Sgr B2M
199	G0.666-0.034	17 47 20.13	-28 23 06.1	1667R	52.15	46.15,61.28	>22.75	A2000	Sgr B2M
200	G359.970-0.457	17 47 20.17	-29 11 58.8	1665	15.5	14,18	10.4	C98	
201	G0.658-0.042	17 47 20.47	-28 23 45.6	1665	67.5	65,77	137	C98	
201	G0.658-0.043	17 47 20.48	-28 23 45.6	1667R	69.23	67.86,73.85	>17.91	A2000	Sgr B2S
201	G0.658-0.043	17 47 20.48	-28 23 45.6	1667L	69.05	47.23,75.94	>26.13	A2000	Sgr B2S
202	G0.670-0.058	17 47 25.61	-28 23 37.6	1612L	67.37	64.85,67.37	>3.84	A2000	Sgr B2
202	G0.670-0.058	17 47 25.61	-28 23 37.6	1612R	67.22	64.79,67.22	>4.09	A2000	Sgr B2
203	G0.546-0.852	17 50 14.52	-28 54 31.5	1665	13.5	3,24	3	C98	
203	G0.547-0.852	17 50 14.53	-28 54 30.8	1667L	12.9	5.34,17.33	>5.22	A2000	RCW 142
203	G0.547-0.852	17 50 14.53	-28 54 30.8	1667R	6.33	4.52,15.27	>3.81	A2000	RCW 142
204	G2.143+0.010	17 50 36.10	-27 05 46.5	1667L	59.26	53.71,62.27	>2.57	A2000	
204	G2.143+0.010	17 50 36.10	-27 05 46.5	1667R	53.69	53.69,62.18	>8.15	A2000	
204	G2.143+0.009	17 50 36.13	-27 05 47.2	1665	59.8	54,64	6	C98	
205	G3.910+0.001	17 54 38.77	-25 34 45.2	1665	17.5	17,20	3.6	C98	
206	IRAS17527-2439	17 55 28.3	-24 36 36	1665R	11.53	8.2,12.2	0.4	EF2007	
207	G5.885-0.392	18 00 30.39	-24 04 01.3	1612	-22	-25,+15	7.1	C99	
207	G5.885-0.392	18 00 30.39	-24 04 04.2	1665	13.9	-44,+19	4.2	C99	
207	G5.885-0.392	18 00 30.58	-24 04 00.9	1720	-13.9		0.17	C2004	
207	G5.886-0.393	18 00 30.63	-24 04 00.9	1667L	9.71	4.94,15.15	>8.99	A2000	
207	G5.886-0.393	18 00 30.63	-24 04 00.9	1667R	10.23	5.18,15.16	>7.86	A2000	
208	G6.795-0.257	18 01 57.72	-23 12 34.6	1665	16.1	13,18	1.8	C98	
209	IRAS18018-2426	18 04 53.1	-24 26 41	1667L	11.05		0.98	EF2007	
209	G6.048-1.447	18 04 53.15	-24 26 42.2	1665	11.2	10,12	7.5	C98	
210	IRAS18024-2119	18 05 25.6	-21 14 59	1665R	-4.05	-9,31	0.69	EF2007	
210	IRAS18024-2119	18 05 25.6	-21 14 59	1667R	-3.75		0.38	EF2007	
211	G9.621+0.196	18 06 14.69	-20 31 32.1	1665	1.4	0,2	6.8	C98	
212	G9.622+0.195	18 06 14.70	-20 31 31.3	1667L	1.48	1.48,7.13	>9.72	A2000	
212	G9.622+0.195	18 06 14.70	-20 31 31.3	1667R	0.64	0.64,7.17	>2.12	A2000	
213	G9.620+0.194	18 06 14.87	-20 31 36.7	1665	22.5	3,25	1.4	C98	
214	G9.619+0.193	18 06 14.92	-20 31 44.0	1665	5.5	5,6	3	C98	
215	G8.669-0.356	18 06 18.99	-21 37 33.1	1720	39.2		1	C2004	
215	G8.669-0.356	18 06 19.01	-21 37 32.8	1665	39.2	38,42	1	C98	
216	G8.683-0.368	18 06 23.46	-21 37 10.2	1665	40	37,45	2.1	C98	
217	IRAS18048-2019	18 07 44.6	-20 18 41	1667L	40.28		0.27	EF2007	
218	G10.480+0.033	18 08 37.87	-19 51 16.1	1665	66	65,67	1	C98	
219	G10.473+0.027	18 08 38.25	-19 51 49.4	1665	51.5	48,69	0.55	C99	
219	G10.473+0.027	18 08 38.33	-19 51 47.9	1720	51.5		0.4	C2004	
220	G10.444-0.018	18 08 44.88	-19 54 37.9	1665	75.5	74,77	0.5	C98	
221	G11.034+0.062	18 09 39.77	-19 21 23.6	1720	21.7		0.45	C2004	
221	G11.034+0.062	18 09 39.86	-19 21 21.2	1665	21.7	20,23	6.7	C99	
222	G10.623-0.383	18 10 28.61	-19 55 49.1	1665	-2	-3,+1	12.3	C98	
222	G10.624-0.385	18 10 28.61	-19 55 49.7	1667L	-0.58	-1.96,2.08	>22.01	A2000	
222	G10.624-0.385	18 10 28.61	-19 55 49.7	1667R	-1.98	-1.98,0.1	>22.37	A2000	
223	IRAS18090-1832	18 11 47.4	-18 29 47	1665R	108.9	103,110	0.7	EF2007	
223	IRAS18090-1832	18 11 47.4	-18 29 47	1667R	106.6		0.49	EF2007	
224	IRAS18089-1732	18 11 51.4	-17 31 29	1667L	33.36		2	EF2007	
224	G12.889+0.489	18 11 51.49	-17 31 30.8	1665	33	31,36	3.6	C98	
225	G12.03-0.04	18 12 03.6	-18 31 53	1665	109.5	103,110	3.1	C98	

226	G11.904-0.141	18 12 11.56	-18 41 29.6	1665	40.5	40,43	6.6	C98	
227	G12.22-0.12	18 12 39.81	-18 24 16.7	1665	27.9	26.81,30.65	>13.30	FC99	
228	G12.210-0.102	18 12 39.89	-18 24 17.3	1665L	21.77		>1.17	A2000	
228	G12.210-0.102	18 12 39.89	-18 24 17.3	1665R	27.04		>0.93	A2000	
229	G12.216-0.117	18 12 44.43	-18 24 23.9	1667L	28.82	26.85,30.58	>11.93	A2000	
229	G12.216-0.117	18 12 44.43	-18 24 23.9	1667R	29.06	27.71,30.69	>4.28	A2000	
229	G12.216-0.119	18 12 44.45	-18 24 24.6	1665	27.9	21,31	11	C98	
230	IRAS18102-1800	18 13 04.4	-18 00 23	1665R	24.4	24,25	0.42	EF2007	
231	G12.680-0.181	18 13 54.75	-18 01 46.4	1667L	64.5	60.58,65.66	>5.51	A2000	W33 B
231	G12.680-0.181	18 13 54.75	-18 01 46.4	1667R	62.52	59.38,66.2	>3.88	A2000	W33 B
232	G12.680-0.183	18 13 54.79	-18 01 47.9	1665	64.5	55,66	10.7	C98	
232	G12.680-0.183	18 13 54.79	-18 01 47.9	1720	63		0.2	C2004	
233	G12.908-0.260	18 14 39.43	-17 52 02.8	1720	32.5		1.2	C2004	
233	G12.908-0.259	18 14 39.47	-17 52 00.2	1667L	39.95	30.84,41.64	>67.18	A2000	W33 A
233	G12.908-0.259	18 14 39.47	-17 52 00.2	1667R	38.96	33,40.45	>9.35	A2000	W33 A
233	G12.908-0.260	18 14 39.53	-17 52 01.1	1665	38	28,42	63.5	C98	
234	IRAS18144-1723	18 17 26.5	-17 22 29	1665L	48.33	48,64	35.9	EF2007	
234	IRAS18144-1723	18 17 26.5	-17 22 29	1667L	61.75		4.8	EF2007	
235	G15.034-0.677	18 20 24.75	-16 11 34.9	1665	21.5	21,24	2.5	C98	
236	G16.59-0.05	18 21 09.10	-14 31 48.5	1665	58.9	58.35,62.74	>2.20	FC99	
237	IRAS18182-1433	18 21 11.0	-14 31 23	1665L	61.55	58,64	0.72	EF2007	
237	IRAS18182-1433	18 21 11.0	-14 31 23	1667L	62.45		0.4	EF2007	
238	G17.639+0.158	18 22 26.13	-13 30 08.0	1720	28.5		<0.15;0.3;0.8	C2004	
239	G17.639+0.155	18 22 26.34	-13 30 12.1	1665L	19.95	19.95,20.92	>3.16	A2000	
239	G17.639+0.155	18 22 26.34	-13 30 12.1	1665R	20.01	20.01,23.31	>2.78	A2000	
240	IRAS18236-1205	18 26 31.7	-12 03 26	1667L	62.45		0.28	EF2007	
241	IRAS18236-1205	18 26 36.2	-12 04 54	1665R	31.09	20,32	0.8	EF2007	
242	G19.61-0.23	18 27 38.09	-11 56 37.2	1665	41.45	39.26,43.65	>4.10	FC99	
243	G20.24+0.07	18 27 44.1	-11 14 54	1665	73.6		2.36	SG2004	
243	G20.24+0.07	18 27 44.1	-11 14 54	1667	72.8		0.74	SG2004	
243	G20.237+0.065	18 27 44.56	-11 14 56.0	1720	75		0.4;0.25;0.28;0.3	C2004	
244	G20.08-0.14	18 28 10.6	-11 28 47	1665	46.6		7.05	SG2004	
244	G20.08-0.14	18 28 10.6	-11 28 47	1667	47.8		0.5	SG2004	
245	G21.57-0.03	18 30 36.5	-10 06 44	1665	119.9		0.23	SG2004	
245	G21.57-0.03	18 30 36.5	-10 06 44	1612	113.9		0.12	SG2004	
246	IRAS18278-1009	18 30 37.9	-10 07 25	1665R	119.7	118,121	0.42	EF2007	
247	G21.87+0.01	18 31 01.9	-09 49 01	1665	22.1		0.38	SG2004	
247	G21.87+0.01	18 31 01.9	-09 49 01	1612	23.8		0.2	SG2004	
248	G22.35+0.06	18 31 45.6	-09 22 44	1665	78		0.91	SG2004	
248	G22.35+0.06	18 31 45.6	-09 22 44	1667	83		0.27	SG2004	
249	IRAS18290-0924	18 31 46.4	-09 22 14	1665R	78.33	76,84	2.3	EF2007	
249	IRAS18290-0924	18 31 46.4	-09 22 14	1667R	78.45		0.34	EF2007	
250	G22.34-0.16	18 32 32.1	-09 29 10	1665	25.4		0.32	SG2004	
251	G22.45-0.17	18 32 45.8	-09 24 06	1665	25.4		7.82	SG2004	
251	G22.45-0.17	18 32 45.8	-09 24 06	1667	33.9		0.17	SG2004	
252	G23.39+0.19	18 33 13.1	-08 23 56	1665	73.5		0.34	SG2004	
252	G23.39+0.19	18 33 13.1	-08 23 56	1667	74.4		0.32	SG2004	
252	G23.39+0.19	18 33 13.1	-08 23 56	1612	75.3		0.24	SG2004	
253	IRAS18310-0825	18 33 36.0	-08 19 46	1667L	88.74	88,89	1.4	EF2007	
254	G23.49+0.08	18 33 47.4	-08 21 37	1665	98.5		0.35	SG2004	
254	G23.49+0.08	18 33 47.4	-08 21 37	1667	88.8		0.2	SG2004	
255	IRAS18316-0602	18 34 25.9	-06 00 01	1665R	39.9	36,46	6	EF2007	
255	IRAS18316-0602	18 34 25.9	-06 00 01	1667L	40.41		3.38	EF2007	
256	G23.26-0.24	18 34 30.8	-08 42 42	1665	56		0.92	SG2004	
256	G23.26-0.24	18 34 30.8	-08 42 42	1667	54.8		1.57	SG2004	
257	G23.44-0.18	18 34 39.0	-08 31 36	1665	106.1		7.91	SG2004	
257	G23.44-0.18	18 34 39.0	-08 31 36	1667	103.3		1.43	SG2004	
257	G23.44-0.18	18 34 39.0	-08 31 36	1720	95.7		0.29	SG2004	
257	G23.44-0.18	18 34 39.0	-08 31 36	1612	103.3		0.19	SG2004	
258	G23.01-0.41	18 34 39.9	-09 00 44	1665	67.6		2.74	SG2004	
258	G23.01-0.41	18 34 39.9	-09 00 44	1667	74.7		4.46	SG2004	
258	G23.01-0.41	18 34 39.9	-09 00 44	1612	78.2		0.2	SG2004	
259	G24.53+0.32	18 34 53.0	-07 19 11	1720	112.6		0.21	SG2004	
260	G23.19-0.38	18 34 54.5	-08 50 04	1665	88.9		1	SG2004	
260	G23.19-0.38	18 34 54.5	-08 50 04	1667	89.7		0.43	SG2004	
260	G23.19-0.38	18 34 54.5	-08 50 04	1720	74.9		0.1	SG2004	
260	G23.19-0.38	18 34 54.5	-08 50 04	1612	78.3		0.31	SG2004	
261	G24.33+0.14	18 35 09.4	-07 34 58	1720	112.9		0.19	SG2004	
262	G24.15-0.01	18 35 20.8	-07 48 48	1665	20.3		0.8	SG2004	
263	G23.97-0.11	18 35 22.9	-08 01 11	1665	72.5		0.29	SG2004	
263	G23.97-0.11	18 35 22.9	-08 01 11	1667	65.8		0.44	SG2004	
263	G23.97-0.11	18 35 22.9	-08 01 11	1612	76.3		0.2	SG2004	
264	G24.51-0.05	18 36 08.7	-07 30 55	1665	108.7		1.5	SG2004	
264	G24.51-0.05	18 36 08.7	-07 30 55	1667	116.3		1.21	SG2004	
264	G24.51-0.05	18 36 08.7	-07 30 55	1612	110.7		0.13	SG2004	
265	G24.79+0.09	18 36 11.9	-07 12 10	1665	112		3.33	SG2004	
265	G24.79+0.09	18 36 11.9	-07 12 10	1667	109		0.83	SG2004	
265	G24.79+0.09	18 36 11.9	-07 12 10	1612	110.4		0.4	SG2004	
266	G25.40+0.11	18 37 18.3	-06 38 38	1665	91.2		0.12	SG2004	
266	G25.40+0.11	18 37 18.3	-06 38 38	1612	95.5		0.3	SG2004	
267	G24.64-0.33	18 37 25.2	-07 31 53	1612	43.1		0.15	SG2004	
268	G25.71+0.04	18 38 03.1	-06 24 32	1665	93.7		7.7	SG2004	
268	G25.71+0.04	18 38 03.1	-06 24 32	1667	94.3		1.51	SG2004	
269	IRAS18360-0537	18 38 42.2	-05 36 25	1665R	102.9	102,106	0.54	EF2007	
270	IRAS18360-0537	18 38 47.2	-05 35 40	1667L	105.3		0.74	EF2007	

271	G25.83-0.18	18 39 04.7	-06 24 17	1667	92.9		0.59	SG2004
272	G27.22+0.14	18 40 29.6	-05 01 09	1665	114.6		1.71	SG2004
272	G27.22+0.14	18 40 29.6	-05 01 09	1667	114.9		0.2	SG2004
273	IRAS18385-0512	18 41 18.2	-05 08 57	1665R	24.87	21,30	1.01	EF2007
274	G28.82+0.37	18 42 35.2	-03 29 26	1665	90.8		0.67	SG2004
275	G28.15+0.00	18 42 40.9	-04 15 26	1665	102.1		2.12	SG2004
275	G28.15+0.00	18 42 40.9	-04 15 26	1667	101		0.25	SG2004
275	G28.15+0.00	18 42 40.9	-04 15 26	1720	102.2		0.71	SG2004
275	G28.15+0.00	18 42 40.9	-04 15 26	1612	98.4		0.1	SG2004
276	G28.147-0.005	18 42 42.57	-04 15 35.5	1665L	102.12		>2.39	A2000
276	G28.147-0.005	18 42 42.57	-04 15 35.5	1665R	100.49	100.49,102.72	>0.54	A2000
277	G28.40+0.07	18 42 54.5	-04 00 04	1665	68.4		0.47	SG2004
277	G28.40+0.07	18 42 54.5	-04 00 04	1612	73		0.45	SG2004
277	G28.40+0.07	18 42 54.5	-04 00 04	1720	77.7		0.65	SG2004
278	G28.19-0.05	18 42 57.8	-04 14 21	1665	96.7		12.97	SG2004
278	G28.19-0.05	18 42 57.8	-04 14 21	1667	97		2.8	SG2004
278	G28.19-0.05	18 42 57.8	-04 14 21	1612	96.6		0.37	SG2004
279	G28.199-0.048	18 42 58.04	-04 13 58.0	1665L	94.92	92.73,100.69	>11.48	A2000
279	G28.199-0.048	18 42 58.04	-04 13 58.0	1665R	94.89	93.98,99.51	>19.23	A2000
279	G28.199-0.048	18 42 58.04	-04 13 58.0	1667L	95.4	92.95,97.16	>1.45	A2000
279	G28.199-0.048	18 42 58.04	-04 13 58.0	1667R	94.21	94.21,98.73	>2.41	A2000
280	G28.86+0.07	18 43 46.22	-03 35 29.8	1665	102.81	102.26,107.74	>9.85	FC99
281	G28.02-0.44	18 44 02.1	-04 34 14	1665	12.9		0.12	SG2004
282	G28.31-0.40	18 44 24.5	-04 17 45	1665	82.9		0.18	SG2004
282	G28.31-0.40	18 44 24.5	-04 17 45	1612	82.8		0.1	SG2004
283	G28.84-0.25	18 44 50.0	-03 45 23	1665	84.9		3.37	SG2004
283	G28.84-0.25	18 44 50.0	-03 45 23	1667	83.5		3.21	SG2004
283	G28.84-0.25	18 44 50.0	-03 45 23	1612	87.8		0.25	SG2004
284	G29.86-0.05	18 45 59.9	-02 45 12	1665	101.5		1.73	SG2004
284	G29.86-0.05	18 45 59.9	-02 45 12	1612	100.6		0.14	SG2004
285	G29.97-0.04	18 46 11.4	-02 39 14	1612	101.5		0.56	SG2004
286	G30.82+0.27	18 46 36.4	-01 45 24	1665	101		4.51	SG2004
286	G30.82+0.27	18 46 36.4	-01 45 24	1667	102.7		1.42	SG2004
286	G30.82+0.27	18 46 36.4	-01 45 24	1720	103.1		0.34	SG2004
286	G30.82+0.27	18 46 36.4	-01 45 24	1612	99		0.22	SG2004
287	IRAS18440-0148	18 46 37.8	-01 44 27	1665R	101.4	99,110	6	EF2007
287	IRAS18440-0148	18 46 37.8	-01 44 27	1667R	102.6		2	EF2007
288	G30.79+0.20	18 46 48.2	-01 48 46	1665	77.8		0.77	SG2004
288	G30.79+0.20	18 46 48.2	-01 48 46	1667	80.3		0.14	SG2004
289	G30.20-0.17	18 47 02.5	-02 30 38	1665	102.1		0.84	SG2004
289	G30.20-0.17	18 47 02.5	-02 30 38	1667	108		0.41	SG2004
290	G30.89+0.17	18 47 07.3	-01 44 15	1665	107.5		0.66	SG2004
290	G30.89+0.17	18 47 07.3	-01 44 15	1667	107		0.4	SG2004
290	G30.89+0.17	18 47 07.3	-01 44 15	1720	90.7		0.28	SG2004
290	G30.89+0.17	18 47 07.3	-01 44 15	1612	98.7		0.5	SG2004
291	G30.59-0.04	18 47 18.7	-02 06 23	1665	37.1		11.97	SG2004
291	G30.59-0.04	18 47 18.7	-02 06 23	1667	37.5		8.71	SG2004
292	G30.589-0.044	18 47 18.81	-02 06 16.9	1665L	37.1	36.09,44.2	>7.62	A2000
292	G30.589-0.044	18 47 18.81	-02 06 16.9	1665R	36.96	36.09,41.38	>7.80	A2000
292	G30.589-0.044	18 47 18.81	-02 06 16.9	1667L	37.5	36.95,39.15	>6.74	A2000
292	G30.589-0.044	18 47 18.81	-02 06 16.9	1667R	37.39	36.64,38.12	>5.27	A2000
293	G31.41+0.31	18 47 34.1	-01 12 58	1665	97.8		2.88	SG2004
293	G31.41+0.31	18 47 34.1	-01 12 58	1667	97.9		12.05	SG2004
293	G31.41+0.31	18 47 34.1	-01 12 58	1720	98		4.52	SG2004
294	G31.412+0.307	18 47 34.25	-01 12 46.1	1665L	101.43	92.55,103.77	>4.63	A2000
294	G31.412+0.307	18 47 34.25	-01 12 46.1	1665R	97.76	92.22,102.96	>2.35	A2000
294	G31.412+0.307	18 47 34.25	-01 12 46.1	1667L	98.07	92.2,105.39	>4.21	A2000
294	G31.412+0.307	18 47 34.25	-01 12 46.1	1667R	97.84	92.2,103.48	>10.47	A2000
295	G30.703-0.069	18 47 36.76	-02 00 54.5	1665L	88.25	85.61,95.79	>2.69	A2000
295	G30.703-0.069	18 47 36.76	-02 00 54.5	1665R	91.17	82.22,96.33	>16.93	A2000
295	G30.703-0.069	18 47 36.76	-02 00 54.5	1667L	87.59	84.72,95.67	>14.90	A2000
295	G30.703-0.069	18 47 36.76	-02 00 54.5	1667R	91.18	85.42,96.42	>11.86	A2000
296	G30.76-0.05	18 47 38.9	-01 57 25	1665	91.2		10.7	SG2004
296	G30.76-0.05	18 47 38.9	-01 57 25	1667	91.1		9.05	SG2004
296	G30.76-0.05	18 47 38.9	-01 57 25	1720	90.3		1.55	SG2004
296	G30.76-0.05	18 47 38.9	-01 57 25	1612	96		2.9	SG2004
297	G31.06+0.09	18 47 45.6	-01 37 19	1665	15.3		1.2	SG2004
297	G31.06+0.09	18 47 45.6	-01 37 19	1720	11.4		0.1	SG2004
298	G30.82-0.05	18 47 46.5	-01 54 24	1665	105.5		9.05	SG2004
298	G30.82-0.05	18 47 46.5	-01 54 24	1667	106		1.63	SG2004
298	G30.82-0.05	18 47 46.5	-01 54 24	1720	91.8		1.18	SG2004
298	G30.82-0.05	18 47 46.5	-01 54 24	1612	96.2		2.12	SG2004
299	G31.15+0.05	18 48 00.3	-01 34 01	1612	40		1.27	SG2004
300	IRAS18454-0158	18 48 01.3	-01 54 34	1665L	39.6	30,44	0.35	EF2007
301	G31.27+0.06	18 48 10.9	-01 26 44	1665	107.2		4.23	SG2004
301	G31.27+0.06	18 48 10.9	-01 26 44	1667	106.9		1.3	SG2004
301	G31.27+0.06	18 48 10.9	-01 26 44	1612	110		0.11	SG2004
302	G31.28+0.06	18 48 11.91	-01 26 38.5	1665	107.19	103.9,108.29	>2.30	FC99
303	G31.57+0.06	18 48 44.3	-01 11 18	1665	97.3		0.34	SG2004
303	G31.57+0.06	18 48 44.3	-01 11 18	1667	98.6		0.12	SG2004
304	G31.24-0.11	18 48 45.08	-01 33 12.7	1665	21.1	20.55,22.74	>3.45	FC99
305	G31.21-0.18	18 48 56.57	-01 36 43.4	1665	-29.45	-29.45,-28.9	>0.50	FC99
306	G32.05+0.06	18 49 38.4	-00 45 29	1665	92.4		2.54	SG2004
306	G32.05+0.06	18 49 38.4	-00 45 29	1667	92.8		0.6	SG2004
306	G32.05+0.06	18 49 38.4	-00 45 29	1612	94.4		0.1	SG2004

307	G32.74-0.08	18 51 21.8	-00 12 13	1665	33.9		1.87	SG2004	
307	G32.74-0.08	18 51 21.8	-00 12 13	1667	34.7		0.88	SG2004	
307	G32.74-0.08	18 51 21.8	-00 12 13	1720	36.7		0.2	SG2004	
308	G32.74-0.07	18 51 21.86	-00 12 06.2	1665	32.26	30.61,39.94	>1.45	FC99	
309	G32.98+0.04	18 51 27.8	+00 04 14	1665	79.3		2.11	SG2004	
309	G32.98+0.04	18 51 27.8	+00 04 14	1667	85.6		1.27	SG2004	
310	IRAS18488+0000	18 51 30.5	+00 03 21	1665R	79.57	79,87	4.52	EF2007	
310	IRAS18488+0000	18 51 30.5	+00 03 21	1667R	77.9		2.66	EF2007	
311	G33.13-0.09	18 52 07.3	+00 08 06	1665	78.5		10.57	SG2004	
311	G33.13-0.09	18 52 07.3	+00 08 06	1667	74.9		0.57	SG2004	
311	G33.13-0.09	18 52 07.3	+00 08 06	1612	75.6		0.26	SG2004	
312	G33.39+0.03	18 52 10.6	+00 25 09	1665	97.1		0.16	SG2004	
312	G33.39+0.03	18 52 10.6	+00 25 09	1612	105.1		0.28	SG2004	
313	G34.25+0.16	18 53 16.7	+01 14 49	1665	58		74.95	SG2004	
313	G34.25+0.16	18 53 16.7	+01 14 49	1667	58.2		95	SG2004	
313	G34.25+0.16	18 53 16.7	+01 14 49	1720	59.2		1.61	SG2004	
314	IRAS18507+0121	18 53 18.2	+01 24 30	1665L	55.78	53,56	2	EF2007	
314	IRAS18507+0121	18 53 18.2	+01 24 30	1667L	53.88		1.1	EF2007	
315	G34.257+0.154	18 53 18.67	+01 14 58.5	1667L	58.64	57.49,62.3	>111.38	A2000	
315	G34.257+0.154	18 53 18.67	+01 14 58.5	1667R	58.49	10.56,66.09	>66.09	A2000	
316	G34.26+0.15	18 53 18.76	+01 14 59.5	1665	56	54.9,63.13	>18.90	FC99	
317	G33.64-0.21	18 53 28.7	+00 31 58	1665	60.2		4.17	SG2004	
317	G33.64-0.21	18 53 28.7	+00 31 58	1667	60.2		0.8	SG2004	
317	G33.64-0.21	18 53 28.7	+00 31 58	1720	60.2		15.87	SG2004	
318	G35.02+0.35	18 54 00.6	+02 01 15	1665	47.6		13.83	SG2004	
318	G35.02+0.35	18 54 00.6	+02 01 15	1667	46.2		0.18	SG2004	
319	IRAS18527+0301	18 54 46.5	+03 05 07	1665R	74.44	72,75	0.21	EF2007	
319	IRAS18527+0301	18 54 46.5	+03 05 07	1667L	73.3		0.16	EF2007	
320	G36.11+0.55	18 55 15.6	+03 04 42	1665	74.3		0.23	SG2004	
321	G35.577-0.029	18 56 22.50	+02 20 27.1	1667L	50.27	48.28,50.27	>11.56	A2000	
321	G35.577-0.029	18 56 22.50	+02 20 27.1	1667R	48.25	48.25,50.25	>0.57	A2000	
321	G35.58-0.03	18 56 22.55	+02 20 28.1	1665	48.9	47.81,49.45	>20.15	FC99	
322	G35.79-0.17	18 57 16.1	+02 27 44	1665	58.3		0.42	SG2004	
322	G35.79-0.17	18 57 16.1	+02 27 44	1667	59.2		0.66	SG2004	
322	G35.79-0.17	18 57 16.1	+02 27 44	1720	58.7		0.1	SG2004	
322	G35.79-0.17	18 57 16.1	+02 27 44	1612	61.9		0.19	SG2004	
323	G36.70+0.09	18 58 00.9	+03 23 30	1665	59.6		0.27	SG2004	
323	G36.70+0.09	18 58 00.9	+03 23 30	1667	60.5		0.27	SG2004	
324	G35.20-0.74	18 58 12.98	+01 40 37.5	1665	36.58	28.9,37.13	>5.10	FC99	
325	G35.197-0.743	18 58 13.02	+01 40 35.2	1665L	35.79	25.11,36.63	>2.02	A2000	
325	G35.197-0.743	18 58 13.02	+01 40 35.2	1665R	28.81	28.81,37.47	>5.39	A2000	
326	G37.02-0.03	18 58 59.9	+03 37 40	1612	78.8		0.1	SG2004	
327	IRAS18566+0408	18 59 08.7	+04 10 21	1665L	83.41	52,92	1	EF2007	
328	IRAS18566+0408	18 59 10.4	+04 13 21	1667L	81.52		0.5	EF2007	
329	G37.55+0.19	18 59 11.6	+04 12 08	1665	85.4		0.69	SG2004	
329	G37.55+0.19	18 59 11.6	+04 12 08	1667	86.4		0.64	SG2004	
329	G37.55+0.19	18 59 11.6	+04 12 08	1612	85.5		0.35	SG2004	
330	G39.10+0.48	19 00 59.5	+05 42 28	1665	21.9		0.13	SG2004	
331	G35.20-1.74	19 01 45.68	+01 13 34.9	1665	42	28.83,45.84	>25.50	FC99	
332	G38.03-0.30	19 01 50.0	+04 23 54	1665	60.4		0.7	SG2004	
332	G38.03-0.30	19 01 50.0	+04 23 54	1667	61.8		0.41	SG2004	
332	G38.03-0.30	19 01 50.0	+04 23 54	1612	60.4		>0.9	SG2004	
333	IRAS19035+0641	19 06 01.6	+06 46 35	1667R	27.33		22.3	EF2007	
333	G40.622-0.137	19 06 01.61	+06 46 35.8	1667L	31.97	25.43,35.55	>18.97	A2000	
333	G40.62-0.14	19 06 01.63	+06 46 36.8	1665	32.65	26.61,35.94	>26.45	FC99	
334	G43.148+0.015	19 10 11.04	+09 05 20.2	1612L	13.2		>2.30	A2000	W49
334	G43.148+0.015	19 10 11.04	+09 05 20.2	1612R	13.82		>2.43	A2000	W49
334	G43.148+0.015	19 10 11.04	+09 05 20.2	1665L	13.65		>7.05	A2000	W49
334	G43.148+0.015	19 10 11.04	+09 05 20.2	1667L	12.72	8.44,12.72	>1.40	A2000	W49
334	G43.148+0.015	19 10 11.04	+09 05 20.2	1667R	12.35	7.89,14.53	>1.16	A2000	W49
335	G43.167+0.010	19 10 13.18	+09 06 12.2	1612L	14.07	13.49,20.54	>7.70	A2000	W49 N
335	G43.167+0.010	19 10 13.18	+09 06 12.2	1612R	14.76	14.07,18.85	>24.11	A2000	W49 N
335	G43.167+0.010	19 10 13.18	+09 06 12.2	1665L	21.04	7.88,23.14	>169.07	A2000	W49 N
335	G43.167+0.010	19 10 13.18	+09 06 12.2	1665R	17.03	7.9,23.19	>108.61	A2000	W49 N
335	G43.167+0.010	19 10 13.18	+09 06 12.2	1667L	19.09	8.29,24.11	>47.24	A2000	W49 N
335	G43.167+0.010	19 10 13.18	+09 06 12.2	1667R	17.05	7.97,24.53	>6.57	A2000	W49 N
336	G43.165-0.028	19 10 21.65	+09 05 02.6	1665L	15.32	12.18,22.38	>64.26	A2000	W49 S
336	G43.165-0.028	19 10 21.65	+09 05 02.6	1665R	16.23	10.7,24.05	>230.48	A2000	W49 S
336	G43.165-0.028	19 10 21.65	+09 05 02.6	1667L	19.25	14.08,19.83	>28.50	A2000	W49 S
336	G43.165-0.028	19 10 21.65	+09 05 02.6	1667R	20.02	13.7,22.58	>16.36	A2000	W49 S
336	G43.165-0.028	19 10 21.68	+09 05 02.4	1720	15		73.7	C2004	
337	IRAS19092+0841	19 11 45.9	+08 46 49	1665R	57.87	54,62	3.45	EF2007	
337	IRAS19092+0841	19 11 46.6	+08 46 19	1667L	60.51		1.75	EF2007	
338	G43.796-0.127	19 11 54.01	+09 35 50.0	1667L	42.52	40.37,44.22	>3.82	A2000	
338	G43.796-0.127	19 11 54.01	+09 35 50.0	1667R	40.16	40.16,43.01	>2.95	A2000	
338	G43.80-0.13	19 11 54.05	+09 35 51.1	1665	41.65	38.35,45.49	>157.05	FC99	
339	G45.07+0.13	19 13 22.06	+10 50 53.5	1665	56.35	53.61,64.04	>29.95	FC99	
339	G45.071+0.134	19 13 22.08	+10 50 54.0	1667L	53.53	53.53,61.45	>6.20	A2000	
339	G45.071+0.134	19 13 22.08	+10 50 54.0	1667R	56.34	54.55,62.93	>3.81	A2000	
340	G45.122+0.133	19 13 27.81	+10 53 37.0	1665L	55.43	54.06,57.08	>6.49	A2000	
340	G45.122+0.133	19 13 27.81	+10 53 37.0	1665R	54.08	52.35,55.86	>4.66	A2000	
340	G45.122+0.133	19 13 27.81	+10 53 37.0	1667L	56.57	52.98,56.57	>12.55	A2000	
340	G45.122+0.133	19 13 27.81	+10 53 37.0	1667R	52.18	52.18,55.31	>2.04	A2000	
341	G45.47+0.13	19 14 07.24	+11 12 16.5	1665	59.55	58.45,59.55	>24.05	FC99	
342	G45.455+0.060	19 14 21.26	+11 09 15.4	1665R	55.09		>0.88	A2000	

343	G45.465+0.047	19 14 25.68	+11 09 25.1	1665L	65.98	62.34,67.24	>18.77	A2000	
343	G45.465+0.047	19 14 25.68	+11 09 25.1	1665R	68.2	62.3,69.76	>4.27	A2000	
344	G45.47+0.05	19 14 25.75	+11 09 25.8	1665	68.19	62.71,69.84	>11.55	FC99	
345	IRAS19118+0945	19 14 29.7	+09 51 47	1665R	61.25	61,71	0.35	EF2007	
345	IRAS19118+0945	19 14 29.7	+09 51 47	1667L	58.9		0.22	EF2007	
346	G48.61+0.02	19 20 31.19	+13 55 24.8	1665	19.45	13.42,20.55	>3.50	FC99	
347	G49.469-0.370	19 23 37.87	+14 29 58.9	1665L	70.46		>0.64	A2000	W51
347	G49.469-0.370	19 23 37.87	+14 29 58.9	1665R	73.82		>2.50	A2000	W51
348	G49.489-0.368	19 23 40.03	+14 31 04.2	1665L	59.89		>1.31	A2000	W51 N
349	G49.491-0.376	19 23 41.96	+14 30 59.4	1720L	64.02		>1.07	A2000	W51
349	G49.491-0.376	19 23 41.96	+14 30 59.4	1720R	64.77		>0.73	A2000	W51
350	G49.488-0.388	19 23 43.83	+14 30 28.3	1720	53.5		2.6	C2004	
351	G49.490-0.387	19 23 43.90	+14 30 34.3	1720	58.1		88	C2004	
351	G49.49-0.39	19 23 43.96	+14 30 35.1	1665	58.55	55.81,67.33	>38.15	FC99	
352	G49.488-0.387	19 23 43.98	+14 30 27.9	1665L	59.26	46.65,69.03	>68.81	A2000	W51 M/S
352	G49.488-0.387	19 23 43.98	+14 30 27.9	1665R	58.26	55.43,71.67	>166.86	A2000	W51 M/S
352	G49.488-0.387	19 23 43.98	+14 30 27.9	1667L	54.16	47.02,70.18	>4.53	A2000	W51 M/S
352	G49.488-0.387	19 23 43.98	+14 30 27.9	1667R	61.94	48.91,72.45	>7.20	A2000	W51 M/S
353	IRAS19217+1651	19 23 57.9	+16 56 42	1665L	-0.21	-2,10	1.35	EF2007	
353	IRAS19217+1651	19 23 57.9	+16 56 42	1667L	6.69		1.22	EF2007	
354	IRAS19374+2352	19 39 37.4	+23 59 53	1665R	37.06	35,40	0.46	EF2007	
354	IRAS19374+2352	19 39 37.4	+23 59 53	1667R	37		0.13	EF2007	
354	IRAS19374+2352	19 39 37.4	+23 59 53	1720R	37.05		0.17	EF2007	
355	IRAS19388+2357	19 41 10.2	+24 03 44	1665L	35.81	34,39	0.32	EF2007	
356	IRAS19410+2336	19 43 12.2	+23 44 03	1665L	20.67	20,23	0.71	EF2007	
357	G70.293+1.601	20 01 45.73	+33 32 45.3	1665L	-19.76	-22.43,-17.55	>11.84	A2000	K3-50
357	G70.293+1.601	20 01 45.73	+33 32 45.3	1665R	-21.27	-22.78,-18.86	>6.05	A2000	K3-50
357	G70.293+1.601	20 01 45.73	+33 32 45.3	1667L	-20.14	-20.81,-20.14	>3.56	A2000	K3-50
357	G70.293+1.601	20 01 45.73	+33 32 45.3	1667R	-21.08		>3.56	A2000	K3-50
358	G70.329+1.590	20 01 54.07	+33 34 13.9	1665L	-14.29	-18.32,-14.29	>0.50	A2000	ON 3
358	G70.329+1.590	20 01 54.07	+33 34 13.9	1665R	-15.7	-16.38,-15.7	>0.80	A2000	ON 3
359	IRAS20062+3550	20 08 12.7	+35 59 20	1665R	-0.77	-1,2.2	0.17	EF2007	
360	G69.540-0.976	20 10 09.05	+31 31 35.2	1665L	2.46	1.12,15.45	>13.66	A2000	ON 1
360	G69.540-0.976	20 10 09.05	+31 31 35.2	1665R	13.11	10.75,13.11	>21.17	A2000	ON 1
360	G69.540-0.976	20 10 09.05	+31 31 35.2	1667L	13.64		>6.18	A2000	ON 1
360	G69.540-0.976	20 10 09.05	+31 31 35.2	1667R	13.28	12.89,13.28	>2.53	A2000	ON 1
361	IRAS20126+4104	20 14 26.06	+41 13 32.63	1665R	-12.7	-16,2	2.37	EF2007	
362	G75.761+0.340	20 21 41.10	+37 25 29.3	1667R	0.75		>1.11	A2000	ON 2 S
363	G75.782+0.343	20 21 43.97	+37 26 38.1	1665L	-3.39	-7.88,2.63	>9.32	A2000	ON 2 N
363	G75.782+0.343	20 21 43.97	+37 26 38.1	1665R	2.54	-5.28,2.54	>36.05	A2000	ON 2 N
363	G75.782+0.343	20 21 43.97	+37 26 38.1	1667L	-4.9	-10.18,4.14	>16.31	A2000	ON 2 N
363	G75.782+0.343	20 21 43.97	+37 26 38.1	1667R	-4.07	-7.95,4.37	>32.74	A2000	ON 2 N
364	IRAS20227+4154	20 24 34.6	+42 06 12	1665L	24.29	10,25	0.8	EF2007	
365	G80.864+0.421	20 36 52.16	+41 36 24.5	1665L	-8.46		>20.15	A2000	
365	G80.864+0.421	20 36 52.16	+41 36 24.5	1665R	-8.46		>25.40	A2000	
366	G81.871+0.781	20 38 36.39	+42 37 34.3	1665L	3.1	0.62,13.69	>27.00	A2000	W75 N
366	G81.871+0.781	20 38 36.39	+42 37 34.3	1665R	12.47	0.63,12.47	>46.04	A2000	W75 N
366	G81.871+0.781	20 38 36.39	+42 37 34.3	1667L	9.33	5.43,9.33	>26.78	A2000	W75 N
366	G81.871+0.781	20 38 36.39	+42 37 34.3	1667R	9.26	6.42,12.87	>19.09	A2000	W75 N
367	G81.745+0.590	20 39 00.38	+42 24 37.1	1665L	3.65		>0.56	A2000	W75
367	G81.745+0.590	20 39 00.38	+42 24 37.1	1665R	2.5	2.5,3.34	>5.20	A2000	W75
368	G81.721+0.571	20 39 00.97	+42 22 48.2	1665L	1.33	-2.8,1.7	>23.33	A2000	W75 S
368	G81.721+0.571	20 39 00.97	+42 22 48.2	1665R	0.65	-4.49,5.19	>26.53	A2000	W75 S
368	G81.721+0.571	20 39 00.97	+42 22 48.2	1667L	-1.94	-1.94,-1.12	>0.93	A2000	W75 S
368	G81.721+0.571	20 39 00.97	+42 22 48.2	1667R	-1.16	-3.48,2.13	>1.55	A2000	W75 S
369	G97.527+3.184	21 32 11.28	+55 53 40.1	1665L	-67.37		>0.14	A2000	
369	G97.527+3.184	21 32 11.28	+55 53 40.1	1665R	-65.78		>2.41	A2000	
370	IRAS22198+6336	22 21 00.7	+63 51 57	1665L	-12.14	-23,-10	2	EF2007	
371	IRAS22198+6336	22 21 37.6	+63 51 47	1667L	-13		3.5	EF2007	
372	IRAS22272+6358	22 28 58.5	+64 15 52	1665L	-12.12	-12,-8	1.1	EF2007	
372	IRAS22272+6358	22 28 58.5	+64 15 52	1667L	-11.96		1.68	EF2007	
373	G109.871+2.114	22 56 17.87	+62 01 48.6	1665L	-11.56	-16.22,-5.07	>40.56	A2000	Cep A
373	G109.871+2.114	22 56 17.87	+62 01 48.6	1665R	-14.24	-14.24,-7.1	>7.31	A2000	Cep A
373	G109.871+2.114	22 56 17.87	+62 01 48.6	1667L	-15.78	-15.78,-3.14	>3.77	A2000	Cep A
373	G109.871+2.114	22 56 17.87	+62 01 48.6	1667R	-14.64	-14.64,-5.25	>4.51	A2000	Cep A
374	G111.533+0.757	23 13 45.02	+61 26 49.3	1665L	-54.33	-60.79,-54.33	>2.82	A2000	
374	G111.533+0.757	23 13 45.02	+61 26 49.3	1665R	-53	-60.7,-53	>2.47	A2000	
375	G111.543+0.777	23 13 45.34	+61 28 10.1	1665L	-59.4	-59.4,-58.14	>39.90	A2000	NGC 7538
375	G111.543+0.777	23 13 45.34	+61 28 10.1	1665R	-59.32	-59.82,-58.19	>11.93	A2000	NGC 7538
375	G111.543+0.777	23 13 45.34	+61 28 10.1	1667L	-59.37		>5.80	A2000	NGC 7538
375	G111.543+0.777	23 13 45.34	+61 28 10.1	1667R	-59.22		>3.59	A2000	NGC 7538

Table 3. Catalogue of 6 cm Interstellar OH masers.

No.	Source name	RA(J2000) (h m s)	DEC(J2000) (^{o} ' ")	Freq. (MHz)	Vpeak (km s^{-1})	Vrange (km s^{-1})	Flux density (Jy)	Ref.	Other name
1	W3-IRS5	02 25 40.7716	+62 05 54.441	4765	-38.95		0.609	SC2005	IRAS02219+6152
2	W3(OH)	02 27 03.7129	+61 52 24.641	4765	-45.01		72.218	SC2005	IRAS02232+6138
3	ORION-IR	05 35 14.48	-05 22 26.6	4660	14.4			GM83	
4	MonR2	06 07 47.8403	-06 22 56.576	4765	10.62		7.722	SC2005	S252-A3
5	IRAS06055+2039	06 08 32.8	+20 39 16	4750	10		1	CM91	S252-A3
5	IRAS06055+2039	06 08 32.8	+20 39 16	4765	10		0.25	CM91	IRAS06055+2039
6	G240.316+0.071	07 44 51.982	-24 07 42	4765	65.0,62.9		0.31,0.17	DE2002	

7	G240.311+0.074	07 44 52.00	-24 07 22	4765	66.7		0.11	DE2002	
8	IRAS11332-6258	11 35 31.04	-63 14 37.3	4765	-12		2.37	S2003	G294.51-1.62
9	IRAS12073-6233	12 09 58.64	-62 49 55.8	4765	31.8		1.4	S97	
10	G309.921+0.479	13 50 41.77	-61 35 09.9	4765	-60.9		0.17	DE2002	
11	G328.304+0.436	15 54 03.94	-53 11 32.2	4765	-91.8		0.12	DE2002	
12	G328.307+0.430	15 54 06.38	-53 11 41.0	4765	-90.5		0.16	DE2002	
13	G328.808+0.633	15 55 48.33	-52 43 06.5	4765	-44.6		0.17	DE2002	
14	G333.135-0.431	16 21 02.80	-50 35 10.1	4765	-51.2		0.14	DE2002	
15	IRAS16183-4958	16 22 09.0	-50 06 00	4765	-50		0.22	CM95	OH333.61-0.22
16	G338.08+0.01	16 35 58.2	-46 35 28	4765	-52.38		1.19	S2003	
17	G338.92+0.55	16 36 54.8	-45 36 14	4765	-61.83		1.46	S2003	
18	G347.63+0.15	17 08 24.8	-39 06 00	4765	-96.34,-95.15		5.71,1.51	S2003	
19	NGC6334N	17 20 53.15	-35 47 12.5	4765	-10.3		0.3	TW70	
20	IRAS17175-3544	17 20 54.75	-35 47 02.4	4765	-10		0.3	CM95	NGC6334F
21	IRAS17233-3606	17 26 44.31	-36 09 27.3	4660	2		1.06	CM95	OH351.78-0.54
22	IRAS17271-3439	17 30 26.59	-34 41 45.1	4765	-20.7		2.52	S2003	OH353.41-0.36
23	IRAS17441-2822	17 47 19.6	-28 23 07	4765	60		1.4	CM91	SGRB2
23	IRAS17441-2822	17 47 19.6	-28 23 07	4750	60		0.5	CM91	SGRB2
23	IRAS17441-2822	17 47 19.6	-28 23 07	4660	60		1.4	CM91	SGRB2
24	G011.90-0.14	18 09 15.2	-18 42 21	4765	41.87		1.85	S2003	
25	IRAS18075-1956	18 10 29.7	-19 55 48	4765	-1		0.4	CM91	W31
26	G11.904-0.141	18 12 11.437	-18 41 29.0	4765	41.8		1	DE2002	
27	W49SW	19 10 10.9430	+09 05 17.598	4765	8.55		0.637	SC2005	
28	IRAS19078+0901	19 10 12.0	+09 06 11	4750	7		0.4	CM91	W49N
28	IRAS19078+0901	19 10 12.0	+09 06 11	4660	7		0.7	CM91	W49N
29	W49N	19 10 13.5173	+09 06 13.911	4765	2.3		0.354	SC2005	IRAS19078+0901
30	W49NW	19 10 14.3	+09 06 24	4765	2.7		0.34	DE2002	
31	W51	19 23 43.9140	+14 30 34.113	4765	57.47		0.151	SC2005	
32	IRAS19598+3324	20 01 45.7259	+33 32 44.970	4765	-20.31		1.535	SC2005	K3-50
33	IRAS20081+3122	20 10 09.23	+31 31 37.4	4765	9.5	-16.5,46.5		B74	ON1
34	W75N	20 38 36.43	+42 37 35.1	4765	13.9		0.28	PG2004	
35	DR21(OH)N	20 39 00.3804	+42 24 37.169	4765	5.04		2.083	SC2005	
36	DR21(OH)	20 39 00.61	+42 22 45.8	4765	-4		2.11	SK2000	
37	IRAS21413+5442	21 43 01.4382	+54 56 17.737	4765	-62.1		0.48	SC2005	
38	IRAS22543+6145	22 56 19.14	+62 01 57.4	4765	-14.7		13.32	SK2000	Cep A
39	NGC7538-IRS1	23 13 45.3501	+61 28 09.745	4765	-59.03		0.492	SC2005	
40	IRAS23116+6111	23 13 45.63	+61 28 17.7	4765	-57.4		3.43	SK2000	NGC7538

Table 4. Catalogue of 5 cm Interstellar OH masers.

No.	Source name	RA(J2000) (h m s)	DEC(J2000) (° ' ")	Freq. (MHz)	Vpeak (km s^{-1})	Vrange (km s^{-1})	Flux density (Jy)	Ref.	Other name
1	IRAS02232+6138	02 27 03.88	+61 52 24.6	6031	-43.33	-47.30,-41.89	49.3	BD97	W3(OH)
1	IRAS02232+6138	02 27 03.88	+61 52 24.6	6035	-43.25	-48.71,-41.9	115.4	BD97	W3(OH)
2	G208.99-19.38	05 35 14.4	-05 22 25	6035		3,23	0.29	CV95	
3	IRAS05392-0214	05 41 44.8	-02 13 23	6035	11.07	11.07,11.15	0.2	BD97	
4	G240.32+0.07	07 44 53.2	-24 07 39	6035		63,64	2.3	CV95	
5	G284.35-0.42	10 24 10.3	-57 52 40	6035		4,9	3.2	CV95	
6	G285.26-0.05	10 31 30.4	-58 02 13	6035		8,12	3.1	CV95	
7	G294.51-1.62	11 35 32.0	-63 14 51	6035		-12	4.6	CV95	
8	G300.97+1.15	12 34 53.9	-61 39 28	6035		-40,-37	4.6	CV95	
9	G305.20+0.02	13 11 20.2	-62 45 26	6035		-38,-31	8.1	CV95	
10	G306.322-0.334	13 21 23.02	-63 00 29.3	6035	-23.5		0.14	C2001	
11	G309.921+0.479	13 50 41.77	-61 35 10.1	6035	-59.7		11.8	C2001	
11	G309.921+0.479	13 50 41.80	-61 35 10.1	6030	-58.1		2.6	C2001	
12	G311.64-0.38	14 06 39.4	-61 58 12	6035		29,35	0.46	CV95	
13	G316.762-0.012	14 44 56.17	-59 48 00.7	6035	-37.5		0.19	C2001	
14	G316.76-0.02	14 44 57.9	-59 48 24	6035		-39	0.28	CV95	
15	G319.398-0.012	15 03 17.41	-58 36 13.3	6035	-12.7		0.15	C2001	
16	G323.46-0.08	15 29 21.0	-56 31 07	6035		-71,-66	17	CV95	
17	G328.30+0.44	15 54 03.1	-53 11 43	6035		-93,-89	1.4	CV95	
18	G328.81+0.63	15 55 47.4	-52 43 08	6035		-47,-42	10.6	CV95	
19	G328.237-0.547	15 57 58.30	-53 59 23.2	6035	-41.0		0.24	C2001	
20	G329.339+0.148	16 00 33.15	-52 44 39.9	6035	-104.2		0.4	C2001	
21	G329.066-0.308	16 01 09.96	-53 16 02.3	6035	-42.7		0.3	C2001	
22	G329.405-0.459	16 03 32.15	-53 09 29.9	6035	-68.5		0.15	C2001	
23	G330.953-0.182	16 09 52.38	-51 54 57.6	6035	-87.9		0.46	C2001	
24	G331.52-0.10	16 12 10.6	-51 28 22	6035		-93,-87	1.6	CV95	
25	G331.54-0.07	16 12 11.0	-51 25 38	6035		-88,-84	4.1	CV95	
26	G332.826-0.549	16 20 10.98	-50 53 12.7	6035	-54.9		1.1	C2001	
27	G333.14-0.43	16 21 03.9	-50 34 52	6035		-57,-49	5.2	CV95	
28	G333.60-0.21	16 22 13.5	-50 06 05	6035		-52	2.1	CV95	
29	G336.358-0.137	16 33 29.19	-48 03 43.7	6035	-75.1		0.3	C2001	
30	G336.36-0.14	16 33 33.5	-48 04 03	6035		-76,-75	0.29	CV95	
31	G336.822+0.028	16 34 38.29	-47 36 32.9	6035	-77.4		0.55	C2001	
32	G336.83+0.02	16 34 41.7	-47 36 32	6035		-78,-77	0.56	CV95	
33	G336.941-0.156	16 35 55.20	-47 38 45.4	6035	-65.7		1.27	C2001	
34	G336.983-0.183	16 36 12.39	-47 37 57.8	6035	-76.2		0.23	C2001	
35	G337.61-0.06	16 38 10.4	-47 05 17	6035		-44,-40	1.18	CV95	
36	G338.28+0.54	16 38 10.8	-46 11 00	6035		-57,-55	1.6	CV95	
37	G337.71-0.05	16 38 30.5	-47 00 45	6035		-57,-48	0.9	CV95	
38	G337.404-0.402	16 38 50.45	-47 28 03.2	6035	-35.6		0.67	C2001	
39	G337.41-0.40	16 38 51.7	-47 28 17	6035		-42,-35	0.36	CV95	

40	G338.08+0.01	16 39 38.8	-46 40 46	6035		-49	0.43	CV95	
41	G338.075+0.012	16 39 39.05	-46 41 28.3	6035	-48.7		0.35	C2001	
42	G338.925+0.557	16 40 33.53	-45 41 37.2	6035	-63.0		0.32	C2001	
43	G339.282+0.136	16 43 43.12	-45 42 08.0	6035	-70.8		0.52	C2001	
44	G339.053-0.315	16 44 48.99	-46 10 13.1	6035	-111.3		0.42	C2001	
45	G339.622-0.121	16 46 05.96	-45 36 44.1	6035	-30.6		0.64	C2001	
46	G339.62-0.12	16 46 08.1	-45 37 08	6035		-35,-30	0.69	CV95	
47	G340.79-0.10	16 50 14.6	-44 42 31	6035		-107,-90	4.4	CV95	
48	G339.884-1.259	16 52 04.60	-46 08 34.0	6030	-37.4		3.3	C2001	
48	G339.884-1.259	16 52 04.61	-46 08 34.0	6035	-37.4		25.5	C2001	
49	G345.01+1.79	16 56 47.6	-40 14 27	6035		-25,-15	8.7	CV95	
50	G343.93+0.12	17 00 11.1	-42 07 24	6035		11,15	3.5	CV95	
51	G344.419+0.044	17 02 08.60	-41 47 10.2	6035	-72.2		0.2	C2001	
52	G345.50+0.35	17 04 22.9	-40 44 23	6035		-23,-22	0.61	CV95	
53	G345.487+0.314	17 04 28.12	-40 46 25.3	6035	-22.1		3.9	C2001	
54	G345.00-0.22	17 05 11.3	-41 29 06	6035		-30,-24	2	CV95	
55	G345.70-0.09	17 06 50.6	-40 51 01	6035		-10,-3	3.4	CV95	
56	G345.407-0.951	17 09 35.40	-41 35 55.0	6035	-26.4		0.26	C2001	
57	G345.407-0.952	17 09 35.43	-41 35 57.1	6035	-16.1		0.29	C2001	
58	G347.63+0.15	17 11 51.1	-39 09 25	6035		-98,-94	5.2	CV95	
59	G348.55-0.98	17 19 20.4	-39 03 54	6035		-14,-10	0.9	CV95	
60	G350.113+0.095	17 19 25.58	-37 10 04.4	6035	-72.1		0.26	C2001	
61	G348.698-1.027	17 19 58.98	-38 58 13.5	6035	-16.3		0.55	C2001	
62	G348.70-1.04	17 20 04.1	-38 58 31	6035		-17,-14	0.39	CV95	
63	G351.42+0.64	17 20 53.5	-35 47 00	6035		-12,-7	140	CV95	
64	G350.686-0.491	17 23 28.63	-37 01 48.5	6035	-15.1		1.09	C2001	
65	G351.58-0.35	17 25 25.4	-36 12 44	6035		-98,-91	7.8	CV95	
66	G351.77-0.54	17 26 42.5	-36 09 18	6035		-9,-2	1.4	CV95	
67	G353.41-0.36	17 30 25.58	-34 41 36.2	6035L	-20.73		19.1	Smits94	
67	G353.41-0.36	17 30 25.58	-34 41 36.2	6035R	-22.291		15.2	Smits94	
67	G353.41-0.36	17 30 25.58	-34 41 36.2	6031L	-21.770		16.2	Smits94	
67	G353.41-0.36	17 30 25.58	-34 41 36.2	6031R	-22.489		24.9	Smits94	
68	G353.410-0.360	17 30 26.18	-34 41 45.5	6030	-22.5		15.5	C2001	
68	G353.410-0.360	17 30 26.18	-34 41 46.0	6035	-20.7		29	C2001	
69	G354.73+0.29	17 31 17.4	-33 14 00	6035		89,95	0.75	CV95	
70	G355.34+0.15	17 33 29.09	-32 47 58.5	6035		17,19	2.3	CV95	
71	G359.14+0.03	17 43 25.68	-29 39 17.4	6035		-2	0.73	CV95	
72	G0.66-0.03	17 47 19.0	-28 22 52	6035		62,73	9.5	CV95	
73	G3.910+0.001	17 54 38.74	-25 34 45.0	6035	17.8		0.32	C2001	
74	G5.885-0.392	18 00 30.36	-24 04 03.1	6035	9.7		0.33	C2001	
75	G8.669-0.356	18 06 19.00	-21 37 32.7	6035	39.4		0.46	C2001	
76	G11.034+0.062	18 09 39.85	-19 21 20.1	6035	23.7		0.45	C2001	
77	G10.623-0.384	18 10 28.65	-19 55 49.6	6035	-0.7		0.42	C2001	
78	G11.90-0.14	18 12 11.56	-18 41 29.6	6035		41,43	3.2	CV95	
79	IRAS18174-1612	18 20 22.43	-16 11 25.3	6031	22.6		0.1	BD97	M17
79	IRAS18174-1612	18 20 22.43	-16 11 25.3	6035	22.63	21.47,23.6	13.7	BD97	M17
80	G15.03-0.68	18 20 24.75	-16 11 34.9	6035		21,24	14	CV95	
81	IRAS18222-1317	18 25 02.27	-13 15 50.8	6035	59.02		0.18	BD97	RAFGL2147
82	G19.486+0.151	18 26 00.39	-11 52 21.9	6035	25.4		2.3	C2001	
83	G20.237+0.065	18 27 44.56	-11 14 54.6	6035	71.6		2.5	C2001	
84	IRAS18274+0112	18 29 57.36	+01 14 45.2	6031	9.52	8.18,10.81	0.1	BD97	S68
84	IRAS18274+0112	18 29 57.36	+01 14 45.2	6035	9.27	9.23,10.22	0.1	BD97	S68
85	G22.435-0.169	18 32 43.83	-09 24 32.8	6035	29.5		0.4	C2001	
86	G22.43-0.17	18 32 45.8	-09 24 43	6035		28,30	0.2	CV95	
87	G28.201-0.049	18 42 58.07	-04 13 57.0	6035	96.1		3.4	C2001	
87	IRAS18403-0417	18 42 58.18	-04 13 59.8	6031	95.05	94.31,95.05	0.4	BD97	OH28.21-0.05
88	G28.20-0.05	18 43 00.3	-04 13 25	6035		93,101	2.7	CV95	
89	G32.744-0.076	18 51 21.88	-00 12 05.5	6035	33.6		0.36	C2001	
90	G34.258+0.153	18 53 18.68	+01 15 00.3	6035	62.1		0.6	C2001	
91	IRAS18507+0110	18 53 19.4	+01 14 34.7	6035	61.94	55.88,62.29	1	BD97	OH34.26+0.15
92	G35.025+0.350	18 54 00.66	+02 01 19.3	6035	45.4		7.5	C2001	
93	IRAS18515+0157	18 54 04.21	+02 01 33.9	6035	45.68	45.39,45.68	4.5	BD97	OH35.03+0.35
94	G35.197-0.743	18 58 13.06	+01 40 37.7	6035	30.3		1	C2001	
95	G35.200-1.736	19 01 45.55	+01 13 33.3	6035	43.2		2.7	C2001	
96	IRAS18592+0108	19 01 46.95	+01 13 07.6	6035	43.35	43.29,44.35	0.4	BD97	W48
97	G40.426+0.700	19 02 39.62	+06 59 12.0	6035	14.4		0.14	C2001	
98	G40.623-0.138	19 06 01.64	+06 46 36.5	6035	32.0		0.2	C2001	
99	G43.149+0.013	19 10 11.05	+09 05 22.1	6035	10.9		1.9	C2001	
100	G43.165+0.013	19 10 12.85	+09 06 12.0	6035	17.0		0.7	C2001	
101	IRAS19078+0901	19 10 15.31	+09 06 08.5	6031	10.45	10.45,13.70	0.3	BD97	W49
101	IRAS19078+0901	19 10 15.31	+09 06 08.5	6035	11.23	-1.86,20.03	0.6	BD97	W49
102	G43.165-0.028	19 10 21.68	+09 05 04.0	6035	13.3		0.56	C2001	
103	IRAS19095+0930	19 11 53.27	+09 35 46.3	6031	40.5		0.1	BD97	
103	G43.795-0.127	19 11 53.97	+09 35 51.8	6035	40.3		0.49	C2001	
104	G45.122+0.133	19 13 27.80	+10 53 39.1	6035	54.2		2.8	C2001	
104	IRAS19111+1048	19 13 27.81	+10 53 33.9	6031	53.67	53.67,53.85	0.2	BD97	
105	IRAS19120+1103	19 14 21.73	+11 09 13.7	6031	66.47	64.92,68.85	0.3	BD97	
105	IRAS19120+1103	19 14 21.73	+11 09 13.7	6035	66.41	64.37,68.77	3.7	BD97	
106	G45.466+0.045	19 14 25.66	+11 09 26.5	6035	66.4		6	C2001	
107	IRAS19201+1400	19 22 26.59	+14 06 36.1	6031	69.28	69.28,69.34	0.4	BD97	
107	IRAS19201+1400	19 22 26.59	+14 06 36.1	6035	67.76	66.94,69.33	2.2	BD97	
108	IRAS19213+1424	19 23 39.95	+14 30 51.1	6031	53.47	53.07,54.29	0.7	BD97	W51e/d
108	IRAS19213+1424	19 23 39.95	+14 30 51.1	6035	57.66	52.40,58.69	1.5	BD97	W51e/d
109	G49.490-0.388	19 23 43.93	+14 30 34.9	6035	57.5		5	C2001	
110	IRAS19598+3324	20 01 45.59	+33 32 44.1	6031	-19.65	-19.06,-19.70	0.2	BD97	K3-50

110	IRAS19598+3324	20 01 45.59	+33 32 44.1	6035	-18.83	-19.69,-18.53	1.1	BD97	K3-50
111	IRAS20081+3122	20 10 09.14	+31 31 34.4	6031	13.91	13.91,14.24	0.9	BD97	ON1
111	IRAS20081+3122	20 10 09.14	+31 31 34.4	6035	14.6	-0.71,15.58	13.1	BD97	ON1
112	IRAS20350+4126	20 36 52.61	+41 36 32.6	6031	-10.82	-11.03,-10.82	0.7	BD97	DR20
112	IRAS20350+4126	20 36 52.61	+41 36 32.6	6035	-9.51	-11.01,-9.51	11.6	BD97	DR20
113	W75N	20 38 36.93	+42 37 37.5	6035	7.83	6.68,8.25	0.5	BD97	
114	W75S(OH)	20 39 00.61	+42 22 48.8	6031	-4.39		0.1	BD97	DR21(OH)
114	W75S(OH)	20 39 00.61	+42 22 48.8	6035	-4.32	-8.78,-2.13	0.3	BD97	DR21(OH)
115	W75S(3)	20 39 03.43	+42 25 53.0	6035	-2.27	-8.75,-2.10	1.1	BD97	
116	IRAS21413+5442	21 43 01.36	+54 56 16.3	6035	-61.37	-61.37,-61.29	1.7	BD97	LDN1084
117	IRAS22176+6303	22 19 18.23	+63 18 46.3	6035	-8.08	-8.24,-8.08	0.4	BD97	S140
118	IRAS22543+6145	22 56 19.14	+62 01 57.4	6031	-8.57	-10.14,-8.57	0.5	BD97	CepA
118	IRAS22543+6145	22 56 19.14	+62 01 57.4	6035	-9.77	-10.04,-8.64	0.6	BD97	CepA
119	IRAS23116+6111	23 13 45.62	+61 28 17.7	6035	-59.1	-60.65,-59.09	1	BD97	NGC7538

Table 5. Catalogue of 2.3 cm Interstellar OH masers.

No.	Source name	RA(J2000) (h m s)	DEC(J2000) (^{o} ' ")	Freq. (MHz)	Vpeak (km s^{-1})	Vrange (km s^{-1})	Flux density (Jy)	Ref.	Other name
1	W3(OH)	02 27 03.88	+61 52 24.57	13441	-43.03		45.3	BD2002	IRAS02232+6138
1	W3(OH)	02 27 03.88	+61 52 24.57	13435L	-45.22			BD2002	
2	G309.921+0.479	13 50 41.77	-61 35 10.1	13441	-57.94		6.33	C2004	
3	G311.596-0.398	14 06 18.35	-62 00 15.3	13441	30.43		0.48	C2004	
4	G328.809+0.633	15 55 48.73	-52 43 05.5	13441	-44.74		0.46	C2004	
5	G329.339+0.148	16 00 33.15	-52 44 39.8	13441	-104.44		0.31	C2004	
6	G331.542-0.066	16 12 09.01	-51 25 47.7	13441	-85.21		0.29	C2004	
7	G336.941-0.156	16 35 55.20	-47 38 45.4	13441	-65.22		0.36	C2004	
8	G345.003-0.224	17 05 11.20	-41 29 07.0	13441	-28.25		0.18	C2004	
9	G11.904-0.141	18 12 11.44	-18 41 29.0	13441	43.00		0.31	C2004	
10	IRAS20081+3122	20 10 09.14	+31 31 34.37	13441	-0.31		0.95	BD2002	ON1
11	IRAS21413+5442	21 43 01.36	+54 56 16.28	13441	-61.47		0.77	BD2002	